Syntheses, Structures, and Electronic and Photophysical Properties of Unsymmetrically Substituted Butadiynediyl and Hexatriynediyl Complexes Derived from $(C_6F_5)(R_3P)_2Pt$, (*p*-tol)$(R_3P)_2Pt$, and $(Ph_3P)Au$ End-Groups

Laura de Quadras,[†] Abigail H. Shelton,[‡] Helene Kuhn,[†] Frank Hampel,[†] Kirk S. Schanze,*[,‡] and John A. Gladysz*[,†,§]

Institut für Organische Chemie and Interdisciplinary Center for Molecular Materials, Friedrich-Alexander-Universität Erlangen-Nürnberg, Henkestrasse 42, 91054 Erlangen, Germany, Department of Chemistry, University of Florida, P.O. Box 117200, Gainesville, Florida 32611, and Department of Chemistry, Texas A&M University, P.O. Box 30012, College Station, Texas 77842-3012

Received May 29, 2008

The CuCl-catalyzed reaction of butadiynyl complex *trans*-$(C_6F_5)(Et_3P)_2Pt(C{\equiv}C)_2H$ (**6**) and *trans*-(*p*-tol)$(Et_3P)_2PtCl$ (**7**) in $HNEt_2$ affords *trans*,*trans*-$(C_6F_5)(Et_3P)_2Pt(C{\equiv}C)_2Pt(PEt_3)_2$(*p*-tol) (**8**; 62%), but similar reactions of *p*-tol$_3$P-substituted coupling partners, or of **6** and *trans*-(*p*-tol)(*p*-tol$_3$P)$_2$PtCl (**4**), are not successful. However, **6** and **4** react under modified conditions (*t*-BuOK, KPF_6, cat. CuCl, THF/methanol) to give *trans*,*trans*-$(C_6F_5)(Et_3P)_2Pt(C{\equiv}C)_2Pt(P$*p*-tol$_3)_2$(*p*-tol) (**9**; 91%). The hexatriynyl complexes *trans*-$(C_6F_5)(R_3P)_2Pt(C{\equiv}C)_3H$ (R = *p*-tol, Et) are treated with **4** and **7**, respectively, under the original or modified conditions. Workups give *trans*,*trans*-$(C_6F_5)(R_3P)_2Pt(C{\equiv}C)_3Pt(PR_3)_2$(*p*-tol) (R = *p*-tol, **12**, 40−63%; Et, **17**, 59%). The reaction of **6** and $ClAu(PPh_3)$ and $KN(SiMe_3)_2$ affords *trans*-$(C_6F_5)(Et_3P)_2Pt(C{\equiv}C)_2Au(PPh_3)$ (**18**, 97%). The CuCl-catalyzed reaction of $(\eta^5\text{-}C_5H_5)W(CO)_3(C{\equiv}C)_2H$ and *trans*-$(C_6F_5)(Et_3P)_2PtCl$ in $HNEt_2$ generates *trans*-$(C_6F_5)(Et_3P)_2Pt(C{\equiv}C)_2W(CO)_3(\eta^5\text{-}C_5H_5)$. The crystal structures of **8**, **9**, **17**, and **18**, or solvates thereof, are determined and analyzed in detail. The square-planar end-groups in the C_4 adducts **8** and **9** define angles of 62.3−34.7°, as opposed to ca. 0° in the C_6 adduct **17**. Both **9** and **18** exhibit phosphorescence from triplet states concentrated on the C_4 segments. Data with **9** in low-temperature glasses suggest two conformers with different end-group−end-group orientations.

Introduction

Our research groups have had an ongoing interest in the synthesis and detailed physical and chemical characterization of metal polyynediyl complexes, $L_yM(C{\equiv}C)_nML_y$.[1−11] Such systems have also attracted the attention of many other investigators.[12−15] These efforts have been motivated by a variety of fundamental and applied objectives, ranging from models for the one-dimensional carbon allotrope carbyne to applications in molecular electronics.

In most but not all[10,11] of our studies, the termini or end-groups have been identical. However, given a large set of end-groups, there are many more possible complexes with unlike termini than like termini. Furthermore, unsymmetrically substituted adducts can provide enhanced driving forces for many phenomena, such as metal-to-metal charge and energy transfer. The diversity intrinsic to such assemblies has been richly exploited by Lapinte in an extensive series of solo and collaborative synthetic, physical, and computational studies.[11,13a,14c,15]

A considerable fraction of our efforts over the past decade have involved symmetrically substituted diplatinum polyynediyl complexes,[2−9] which are most often prepared by the Hay oxidative homocoupling protocol exemplified in Scheme 1 (top). These endeavors have encompassed systems that (a) extend to as many as 28 sp carbon atoms,[3] (b) are "insulated" by a double helix of sp^3 carbon chains,[4] (c) contain "bundled" arrays of

* To whom correspondence should be addressed. Phone: 979-845-1399 (J.A.G.); 352-392-9133 (K.S.S.). Fax: 979-845-5629 (J.A.G.); 202-513-8648 (K.S.S). E-mail: gladysz@mail.chem.tamu.edu (J.A.G.); kschanze@chem.ufl.edu (K.S.S).

[†] Universität Erlangen-Nürnberg.

[‡] University of Florida.

[§] Texas A&M University.

(1) (a) Brady, M.; Weng, W.; Zhou, Y.; Seyler, J. W.; Amoroso, A. J.; Arif, A. M.; Böhme, M.; Frenking, G.; Gladysz, J. A. *J. Am. Chem. Soc.* **1997**, *119*, 775. (b) Dembinski, R.; Bartik, T.; Bartik, B.; Jaeger, M.; Gladysz, J. A. *J. Am. Chem. Soc.* **2000**, *122*, 810. (c) Meyer, W. E.; Amoroso, A. J.; Horn, C. R.; Jaeger, M.; Gladysz, J. A. *Organometallics* **2001**, *20*, 1115. (d) Horn, C. R.; Gladysz, J. A. *Eur. J. Inorg. Chem.* **2003**, *9*, 2211.

(2) Mohr, W.; Stahl, J.; Hampel, F.; Gladysz, J. A. *Chem.−Eur. J.* **2003**, *9*, 3324.

(3) Zheng, Q.; Bohling, J. C.; Peters, T. B.; Frisch, A. C.; Hampel, F.; Gladysz, J. A. *Chem.−Eur. J.* **2006**, *12*, 6486.

(4) Owen, G. R.; Hampel, F.; Gladysz, J. A. *Organometallics* **2004**, *23*, 5893.

(5) Zheng, Q.; Hampel, F.; Gladysz, J. A. *Organometallics* **2004**, *23*, 5896.

(6) (a) Stahl, J.; Mohr, W.; de Quadras, L.; Peters, T. B.; Bohling, J. C.; Martín-Alvarez, J. M.; Owen, G. R.; Hampel, F.; Gladysz, J. A. *J. Am. Chem. Soc.* **2007**, *129*, 8282. (b) de Quadras, L.; Bauer, E. B.; Mohr, W.; Bohling, J. C.; Peters, T. B.; Martín-Alvarez, J. M.; Hampel, F.; Gladysz, J. A. *J. Am. Chem. Soc.* **2007**, *129*, 8296. (c) de Quadras, L.; Bauer, E. B.; Stahl, J.; Zhuravlev, F.; Hampel, F.; Gladysz, J. A. *New J. Chem.* **2007**, *31*, 1594. (d) Owen, G. R.; Stahl, J.; Hampel, F.; Gladysz, J. A. *Chem.−Eur. J.* **2008**, *14*, 73.

(7) Stahl, J.; Bohling, J. C.; Peters, T. B.; de Quadras, L.; Gladysz, J. A. *Pure Appl. Chem.* **2008**, *80*, 459.

(8) Silverman, E. E.; Cardolaccia, T.; Zhao, X.; Kim, K.-Y.; Haskins-Glusac, K.; Schanze, K. S. *Coord. Chem. Rev.* **2005**, *249*, 1491.

(9) Farley, R. T.; Zheng, Q.; Gladysz, J. A.; Schanze, K. S. *Inorg. Chem.* **2008**, *47*, 2955.

10.1021/om800493x CCC: $40.75
Publication on Web 09/13/2008

Scheme 1. Previously Investigated Coupling Routes to Symmetrically Substituted Diplatinum Polyynediyl Complexes

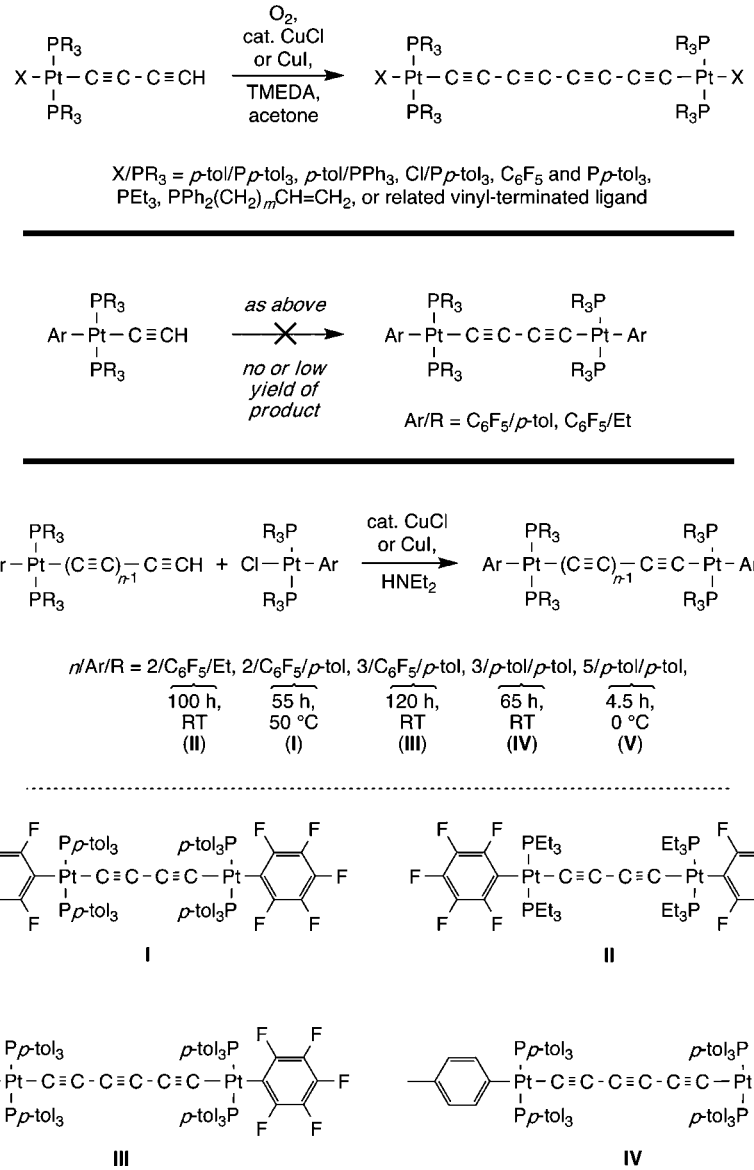

parallel sp chains,[5] and (d) have been longitudinally extended to $PtC_xPtC_xPtC_xPt$ species.[6] In all of these cases, the end-groups have been identical.

Accordingly, we set out to test various approaches to achieving unsymmetrically substituted diplatinum polyynediyl complexes or heterobimetallic analogues with one non-platinum end-group and briefly probe their structural, electronic, and photophysical properties. These efforts are narrated below, and additional details are available elsewhere.[16]

Results

1. Syntheses of Diplatinum Butadiynediyl Complexes. As summarized in Scheme 1 (top), many diplatinum octatetraynediyl complexes can be prepared by Hay homocouplings of the corresponding monoplatinum butadiynyl complexes.[2,3,6b,c,7] In contrast, analogous reactions of the ethynyl complexes *trans*-

(10) (a) Weng, W.; Bartik, T.; Brady, M.; Bartik, B.; Ramsden, J. A.; Arif, A. M.; Gladysz, J. A. *J. Am. Chem. Soc.* **1995**, *117*, 11922. (b) Falloon, S. B.; Szafert, S.; Arif, A. M.; Gladysz, J. A. *Chem.*−*Eur. J.* **1998**, *4*, 1033.

(11) (a) Paul, F.; Meyer, W. E.; Toupet, L.; Jiao, H.; Gladysz, J. A.; Lapinte, C. *J. Am. Chem. Soc.* **2000**, *122*, 9405. (b) Jiao, H.; Costuas, K.; Gladysz, J. A.; Halet, J.-F.; Guillemot, M.; Toupet, L.; Paul, F.; Lapinte, C. *J. Am. Chem. Soc.* **2003**, *125*, 9511. (c) Szafert, S.; Paul, F.; Meyer, W. E.; Gladysz, J. A.; Lapinte, C. *C. R. Chem.* **2008**, 11, 693.

(12) Review literature:(a) Bruce, M. I.; Low, P. J. *Adv. Organomet. Chem.* **2004**, *50*, 179. (b) Szafert, S.; Gladysz, J. A. *Chem. Rev* **2003**, *103*, 4175; **2006**, *106*, PR1−PR33.

(13) Selected lead papers to a now-immense literature: (a) Lapinte, C. *J. Organomet. Chem.* **2008**, *693*, 793. (b) Bruce, M. I.; Low, P. J.; Costuas, K.; Halet, J.-F.; Best, S. P.; Heath, G. A. *J. Am. Chem. Soc.* **2000**, *122*, 1949. (c) Xu, G.-L.; Zou, G.; Ni, Y.-H.; DeRosa, M. C.; Crutchley, R. J.; Ren, T. *J. Am. Chem. Soc.* **2003**, *125*, 10057. (d) Akita, M.; Sakurai, A.; Chung, M.-C.; Moro-oka, Y. *J. Organomet. Chem.* **2003**, *670*, 2. (e) Venkatesan, K.; Fox, T.; Schmalle, H. W.; Berke, H. *Organometallics* **2005**, *24*, 2834. (f) Qi, H.; Gupta, A.; Noll, B. C.; Snider, G. L.; Lu, Y.; Lent, C.; Fehlner, T. P. *J. Am. Chem. Soc.* **2005**, *127*, 15218.

(14) Heterobimetallic polyynediyl complexes especially relevant to this study: (a) Antonova, A. B.; Bruce, M. I.; Ellis, B. G.; Gaudio, M.; Humphrey, P. A.; Jevric, M.; Melino, G.; Nicholson, B. K.; Perkins, G. J.; Skelton, B. W.; Stapleton, B.; White, A. H.; Zaitseva, N. N. *Chem. Commun.* **2004**, 960. (b) Bruce, M. I.; Hall, B. C.; Low, P. J.; Smith, M. E.; Skelton, B. W.; White, A. H. *Inorg. Chim. Acta* **2000**, *300*−*302*, 633. (c) Bruce, M. I.; Costuas, K.; Davin, T.; Ellis, B. G.; Halet, J.-F.; Lapinte, C.; Low, P. J.; Smith, M. E.; Skelton, B. W.; Toupet, L.; White, A. H. *Organometallics* **2005**, *24*, 3864. (d) Bruce, M. I.; Jevric, M.; Skelton, B. W.; Smith, M. E.; White, A. H.; Zaitseva, N. N. *J. Organomet. Chem.* **2006**, *691*, 361.

(15) Other literature especially relevant to this study: (a) Coat, F.; Guillevic, M.-A.; Toupet, L.; Paul, F.; Lapinte, C. *Organometallics* **1997**, *16*, 5988. (b) Coat, F.; Guillemot, M.; Paul, F.; Lapinte, C. *J. Organomet. Chem.* **1999**, *578*, 76.

(16) de Quadras, L. Doctoral Dissertation, Universität Erlangen-Nürnberg, 2006.

Scheme 2. Attempted Syntheses of Unsymmetrically Substituted Diplatinum Butadiynediyl Complexes

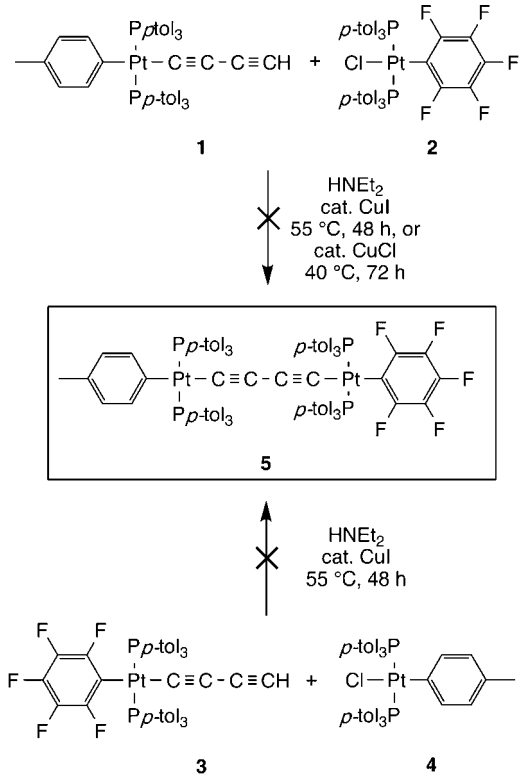

1 **2** **3** **4** **5**

$(C_6F_5)(R_3P)_2PtC{\equiv}CH$ (Scheme 1, middle) do not yield significant quantities of butadiynediyl complexes.[7,17] Possible underlying steric and electronic factors are analyzed below. However, two such complexes have been isolated in high yields by Hagihara heterocouplings[18] of the butadiynyl complexes *trans*-$(Ar)(R_3P)_2Pt(C{\equiv}C)_2H$ and chloride complexes *trans*-$(Ar)(R_3P)_2$-PtCl, using the basic solvent $HNEt_2$ and a catalytic amount of CuCl or CuI (**I** and **II** in Scheme 1, bottom).[2,7,19]

Thus, as summarized in Scheme 2, equimolar quantities of the *p*-tolyl- and pentafluorophenyl-substituted butadiynyl and chloride complexes *trans*-(*p*-tol)(*p*-$tol_3P)_2Pt(C{\equiv}C)_2H$ (**1**)[3] and *trans*-(C_6F_5)(*p*-$tol_3P)_2PtCl$ (**2**),[2] or the "opposite" combination *trans*-(C_6F_5)(*p*-$tol_3P)_2Pt(C{\equiv}C)_2H$ (**3**)[2] and *trans*-(*p*-tol)(*p*-$tol_3P)_2PtCl$ (**4**),[3] were combined under various Hagihara conditions. However, NMR monitoring showed the concomitant decomposition of one or both reaction partners, and only traces of the target complex *trans*,*trans*-(*p*-tol)(*p*-$tol_3P)_2Pt(C{\equiv}C)_2Pt(P$*p*-$tol_3)_2(C_6F_5)$ (**5**) could be detected by mass spectrometry. Additional details are supplied elsewhere.[16]

Structural data (below) suggest that the effective steric bulk of Et_3P ligands in symmetrically substituted diplatinum polyynediyl complexes is much less than that of Ar_3P ligands.[6d] Thus, a reaction analogous to that of **3** and **4** in Scheme 2 was conducted, but with the Et_3P complexes *trans*-$(C_6F_5)(Et_3P)_2$-$Pt(C{\equiv}C)_2H$ (**6**)[7] and *trans*-(*p*-tol)$(Et_3P)_2Pt(Cl)$ (**7**).[7] As shown in Scheme 3 (top), the target butadiynediyl complex *trans*,*trans*-$(C_6F_5)(Et_3P)_2Pt(C{\equiv}C)_2Pt(PEt_3)$(*p*-tol) (**8**) could be isolated as an off-white powder in 62% yield after workup.

Scheme 3. Syntheses of Unsymmetrically Substituted Diplatinum Butadiynediyl Complexes

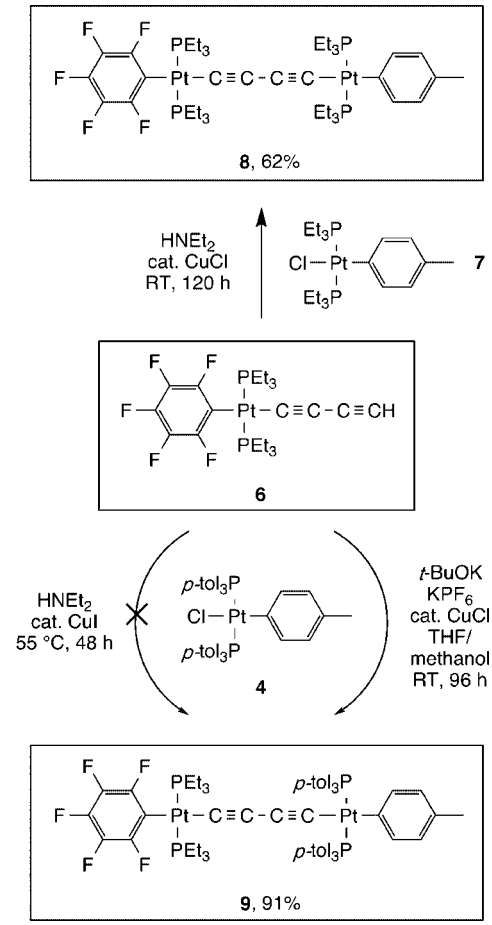

8, 62% **7** **6** **4** **9**, 91%

Table 1. Cyclic Voltammetry Data[a]

complex	$E_{p,a}$ [V]	$E_{p,c}$ [V]	$E°$ [V]	ΔE [V]	$i_{c/a}$
8	0.845	0.772	0.809	73	0.91
9	0.827	0.757	0.792	70	0.78
12	1.040	0.963	1.001	77	0.27
17	1.011	0.919	0.965	92	0.25
18	1.268				
I[b]	0.940	0.862	0.901	78	0.98
II[c]	1.035	0.957	0.996	78	0.91
III[d]	1.156	1.066	1.111	90	0.71
IV[e]	0.855				

[a] Conditions: $3-5 \times 10^{-4}$ M, *n*-$Bu_4N^+BF_4^-/CH_2Cl_2$ at 22.5 ± 1 °C; Pt working and counter electrodes, potential vs Ag wire pseudo-reference; scan rate 100 mV s^{-1}; ferrocene = 0.46 V. [b] Data from ref 22. [c] Data from ref 17. [d] Data from ref 6d. [e] Data from ref 3.

Complex **8** and all isolable new compounds below were characterized by IR, NMR (^1H, ^{13}C, ^{31}P), and UV−visible spectroscopy, mass spectrometry, cyclic voltammetry, DSC, TGA, and microanalysis. The cyclic voltammetry results are provided in Table 1, and the other data in the Experimental Section. All complexes were stable for extended periods in air, with TGA traces showing no appreciable mass losses below 200 °C. The ^{13}C and ^{31}P NMR spectra of the diplatinum complexes resembled hybrids of the symmetrically substituted complexes **I**−**IV**. The $^1J_{PPt}$ values (2406−2987 Hz), which are diagnostic of stereochemistry,[20] confirmed the formation of *trans* isomers.

(17) Stahl, J. Doctoral Dissertation, Universität Erlangen-Nürnberg, 2003.

(18) (a) Sonogashira, K.; Fujikura, Y.; Yatake, T.; Toyoshima, N.; Takahashi, S.; Hagihara, N. *J. Organomet. Chem.* **1978**, *145*, 101. (b) Ogawa, H.; Onitsuka, K.; Joh, T.; Takahashi, S.; Yamamoto, Y.; Yamakazi, H. *Organometallics* **1988**, *7*, 2257, and earlier papers cited therein.

(19) Curiously, this heterocoupling fails with *trans*-(*p*-tol)(*p*-$tol_3P)_2Pt$ end-groups (cat. CuI or CuCl at RT to 40 °C): Zheng, Q. Unpublished data including final research report, Universität Erlangen-Nürnberg, 2006.

(20) Grim, S. O.; Keiter, R. L.; McFarlane, W. *Inorg. Chem.* **1967**, *6*, 1133.

Given this success, mixed Et_3P/Ar_3P systems were targeted. As shown in Scheme 3 (bottom), an analogous reaction of **6** and **4** did not afford detectable quantities of the butadiynyl complex *trans*,*trans*-$(C_6F_5)(Et_3P)_2Pt(C{\equiv}C)_2Pt(P\textit{p}\text{-}tol_3)_2(\textit{p}\text{-}tol)$ (**9**). However, couplings of terminal alkynes and butadiynyl complexes with metal halides have also been effected using KPF_6/*t*-BuOK in place of $HNEt_2$.[11a,c,15] Thus, the reaction of **6** and **4** was carried out in the presence of a slight excess of *t*-BuOK and KPF_6 and a catalytic amount of CuCl in a mixture of THF and methanol. The target complex **9** was isolated as a pale yellow solid in 91% yield after workup.

2. Syntheses of Diplatinum Hexatriynediyl Complexes. Analogous routes to diplatinum hexatriynediyl complexes were investigated next. Since monoplatinum hexatriynyl complexes are labile and store poorly, they were generated in situ from the corresponding triethylsilylhexatriynyl complexes by an established protocol involving wet *n*-$Bu_4N^+F^-$ in CH_2Cl_2.[2,3] As shown in Scheme 4 (bottom), the *p*-tolyl-substituted hexatriynyl complex *trans*-(*p*-tol)(*p*-$tol_3P)_2Pt(C{\equiv}C)_3H$ (**11**)[3] was combined with the pentafluorophenyl-substituted chloride complex **2** under Hagihara conditions. However, the target complex *trans*,*trans*-(*p*-tol)(*p*-$tol_3P)_2Pt(C{\equiv}C)_3Pt(P\textit{p}\text{-}tol_3)_2(C_6F_5)$ (**12**) could not be detected by NMR or mass spectrometry. NMR data suggested that **11** decomposed faster than it underwent heterocoupling.[16]

The "opposite" reactant combination was therefore investigated. As shown in Scheme 4 (top), the pentafluorophenyl-substituted butadiynyl complex *trans*-$(C_6F_5)(\textit{p}\text{-}tol_3P)_2Pt(C{\equiv}C)_3H$ (**14**)[2] was combined with the *p*-tolyl-substituted chloride complex **4** under analogous conditions. Workup gave the hexatriynediyl complex **12** as a yellow powder in 40% yield. When the modified protocol used for **9** in Scheme 3 was employed (KPF_6/*t*-BuOK/methanol/THF in place of $HNEt_2$), the yield increased to 63%. This protocol was also employed in a sequence conducted with the Et_3P complexes *trans*-$(C_6F_5)(Et_3P)_2Pt(C{\equiv}C)_3SiEt_3$ (**15**)[7] and **7** (Scheme 4, top). Workup gave the target complex *trans*,*trans*-$(C_6F_5)(Et_3P)_2Pt(C{\equiv}C)_3Pt(PEt_3)_2(\textit{p}\text{-}tol)$ (**17**) as a yellow powder in 59% yield.

3. Syntheses of Heterobimetallic Polyynediyl Complexes. Under appropriate conditions, gold polyynyl complexes readily couple with $I(C{\equiv}C)_nI$ or $L_yM(C{\equiv}C)_nI$ species.[14a,21] Hence, they constitute valuable building blocks for the synthesis of compounds with longer sp carbon chains. Accordingly, efforts were directed at $Pt(C{\equiv}C)_nAu$ assemblies, which have a very limited literature.[22] A variety of recipes have been used to attach $(Ar_3P)Au$ end-groups to terminal alkynes.[14d] As shown in Scheme 5 (top), the sequential treatment of the butadiynyl complex **6** with the chloride complex $(Ph_3P)AuCl$[23] and then the base $KN(SiMe_3)_2$ gave the target complex *trans*-$(C_6F_5)(Et_3P)_2Pt(C{\equiv}C)_2Au(PPh_3)$ (**18**) as a yellow powder in 97% yield after workup. Reactions under Hagihara conditions gave complex mixtures of products. In accord with literature precedent,[14d] The Au*CC* ^{13}C NMR signals of **18** were strongly coupled to phosphorus (J_{CP} = 143 and 30 Hz), with the former considerably downfield of the PtC signal (116.6 vs 93.7 ppm).

Scheme 4. Syntheses of Unsymmetrically Substituted Diplatinum Hexatriynediyl Complexes

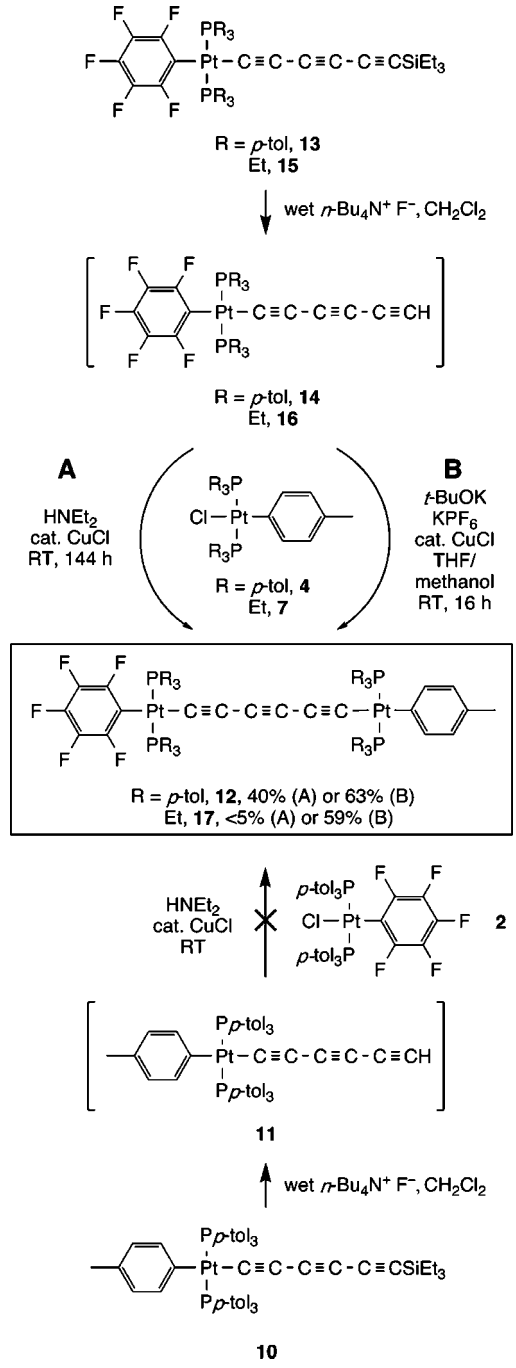

The tungsten chloride complex $(\eta^5\text{-}C_5H_5)(CO)_3WCl$ (**21**)[24] reacts with terminal alkynes and butadiyne under Hagihara conditions to give alkynyl complexes.[25] However, as shown in Scheme 5 (bottom), analogous reactions with the butadiynyl complex **6** did not give detectable quantities of the target complex *trans*-$(C_6F_5)(Et_3P)_2Pt(C{\equiv}C)_2W(CO)_3(\eta^5\text{-}C_5H_5)$ (**22**). The tungsten butadiynyl complex $(\eta^5\text{-}C_5H_5)(CO)_3W(C{\equiv}C)_2H$ (**23**)[25] similarly condenses with various metal chloride complexes under Hagihara-type conditions.[14c] Thus, as shown in Scheme 5 (bottom), the reaction of **23** and the platinum chloride complex **2** was carried out under standard conditions. Alumina filtration gave **22** as a yellow powder, as assigned by a parent

(21) Antonova, A. B.; Bruce, M. I.; Humphrey, P. A.; Gaudio, M.; Nicholson, B. K.; Scoleri, N.; Skelton, B. W.; White, A. H.; Zaitseva, N. N. *J. Organomet. Chem.* **2006**, *691*, 4694.

(22) (a) Bruce, M. I.; Costuas, K.; Halet, J.-F.; Hall, B. C.; Low, P. J.; Nicholson, B. K.; Skeleton, B. W.; White, A. H. *J. Chem. Soc., Dalton Trans.* **2002**, 383. (b) Bruce, M. I.; Hall, B. C.; Skeleton, B. W.; Smith, M. E.; White, A. H. *J. Chem. Soc., Dalton Trans.* **2002**, 995. (c) See also: Vicente, J.; Chicote, M.-T.; Alvarez-Falcón, M. M. *Organometallics* **2005**, *24*, 2764.

(23) Bruce, M. I.; Nicholson, B. K.; Bin Shawkataly, O. *Inorg. Synth.* **1989**, *26*, 324.

(24) Hoffman, N. W. *Inorg. Chim. Acta* **1984**, *88*, 59.

(25) Bruce, M. I.; Ke, M.; Low, P. J.; Skelton, B. W.; White, A. H. *Organometallics* **1998**, *17*, 3539.

Scheme 5. Syntheses of Heterobimetallic Butadiynediyl Complexes

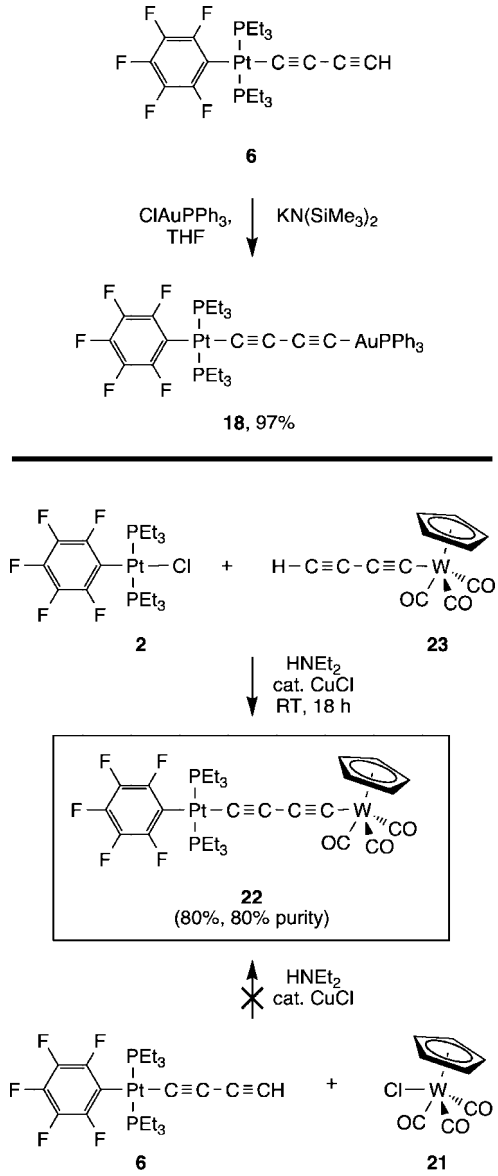

ion in the mass spectrum, a ^{31}P NMR spectrum showing one main signal (12.8 ppm, $^{1}J_{PPt} = 2431$ Hz, 80% of total integral), and a ^{13}C NMR spectrum with peaks appropriate for WC≡ and PtC≡ signals (116.4, 93.9 ppm). However, all attempts to further purify **22** by column chromatography or crystallization were unsuccessful.

4. Crystal Structures. Crystals of **8**, **9**, **17**, and **18**, or solvates thereof, that were suitable for X-ray diffraction could be obtained. The structures were solved as described in the Experimental Section and Table 2. That of **8** was disordered over two positions in which the pentafluorophenyl and *p*-tolyl ligands were nearly coincident, but occupancy could be refined to a 73:27 ratio. Thermal ellipsoid, space-filling, and other representations of the molecular structures are depicted in Figures 1−4, and packing diagrams are provided elsewhere.[16] Key metrical parameters are summarized in Tables 3 and 4. End-group/end-group angles were quantified by two sets of planes (Table 3) as described in previous papers.[2,3,6] Two independent molecules of **18** were present in the unit cell, but exhibited only minor differences in the conformations of the end-groups.

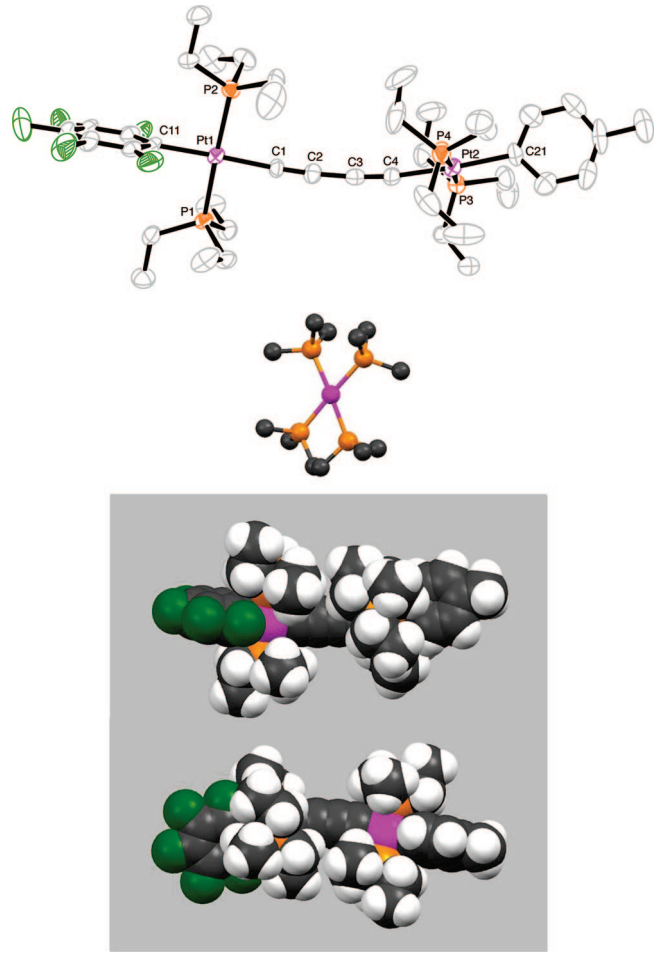

Figure 1. Thermal ellipsoid (top; 50% probability level), Newman (middle), and space-filling (bottom) representations of **8**.

The bond lengths and angles in **8**, **9**, **17**, and **18** were unexceptional and close to those of symmetrically substituted diplatinum analogues.[2−6] The C≡C and C−C bond lengths fell in the typical ranges of 1.119−1.224 and 1.356−1.400 Å, respectively. The sp carbon chains were, as is normal for polyynes[12c] and other compounds in this series,[2−6,26] slightly curved. This feature is analyzed in greater detail elsewhere,[16] and additional structural properties are discussed below.

5. Photophysics of the PtC$_4$Pt′ and PtC$_4$Au Complexes 9 and 18. The butadiynediyl complexes **9** and **18**, which feature one common end-group, were selected for a comparative photophysical study. Absorption, emission, and emission excitation spectra were first recorded, as depicted in Figure 5. The absorption spectra were obtained from 2-methyltetrahydrofuran (MTHF) solutions at ambient temperature, whereas the emission experiments were conducted at 80 K in a MTHF glass.

In accord with earlier computational data,[27] the UV absorptions were presumed to be dominated by π,π^* transitions of the butadiynediyl segments. Close comparison of the spectra showed that absorption of the diplatinum complex **9** extended

(26) (a) Bohling, J. C.; Peters, T. B.; Arif, A. M.; Hampel, F.; Gladysz, J. A. In *Coordination Chemistry at the Turn of the Century*; Ondrejoviç, G., Sirota, A. Eds.; Slovak Technical University Press: Bratislava, Slovakia, 1999; pp 47−52. (b) Peters, T. B.; Zheng, Q.; Stahl, J.; Bohling, J. C.; Arif, A. M.; Hampel, F.; Gladysz, J. A. *J. Organomet. Chem.* **2002**, *641*, 53. (c) Mohr, W.; Peters, T. B.; Bohling, J. C.; Hampel, F.; Arif, A. M.; Gladysz, J. A. *C. R. Chem.* **2002**, *5*, 111.

(27) Zhuravlev, F.; Gladysz, J. A. *Chem.−Eur. J.* **2004**, *10*, 6510.

Table 2. Summary of Crystallographic Data[a]

	8	**9**·CH_2Cl_2	**17**	**18**·$(C_7H_8)_{0.5}$
empirical formula	$C_{41}H_{71}F_5P_4Pt_2$	$C_{72}H_{81}Cl_2F_5P_4Pt_2$	$C_{43}H_{67}F_5P_4Pt_2$	$C_{43.50}H_{49}AuF_5P_3Pt$
fw	1173.04	1626.33	1193.03	1151.79
cryst syst	monoclinic	triclinic	monoclinic	triclinic
space group	$P2_1/n$	$P\bar{1}$	$P2_1/n$	$P\bar{1}$
unit cell dimen				
a [Å]	9.0267(4)	11.97090(10)	13.5959(2)	12.6692(4)
b [Å]	36.3908(2)	17.7039(2)	11.4504(2)	13.6709(3)
c [Å]	14.5404(8)	18.2489(2)	30.6720(5)	25.2832(8)
α [deg]	90	78.3350(10)	90	78.011(2)
β [deg]	96.838(2)	88.1700(10)	90.788(1)	87.011(1)
γ [deg]	90	72.1490(10)	90	89.648
V [Å^3]	4742.4(3)	3481.30(6)	4774.52(13)	4277.6(2)
Z	4	4	4	4
ρ_{calcd} [Mg m^{-3}]	1.643	1.551	1.660	1.788
μ [mm^{-1}]	6.074	4.236	6.035	6.856
F(000)	2312	1616	2344	2228
cryst size, mm	0.20 × 0.20 × 0.20	0.25 × 0.20 × 0.15	0.20 × 0.20 × 0.10	0.20 × 0.20 × 0.01
θ range [deg]	1.12 to 27.45	1.53 to 27.48	1.33 to 27.51	1.52 to 25.04
index ranges (h,k,l)	−11,11; −47,43; −18,18	−15,15; −21,22; −23,23	−17,17; −14,14; −39,39	−15,15; −15,16; −30,30
no. reflns collected	11853	30543	20405	24331
no. indep reflns	8928 [R(int) = 0.0258]	15 929 [R(int) = 0.0219]	10 873 [R(int) = 0.0251]	14 421 [R(int) = 0.0386]
no. reflns [$I > 2\sigma(I)$]	6339	13 090	7454	8280
max. and min. transmn	0.3763 and 0.3763	0.5691 and 0.4173	0.5836 and 0.3782	0.9346 and 0.3409
no. data/restraints/params	8928/2/500	15 929/25/777	10 873/0/500	14 421/0/1003
goodness-of-fit on F^2	1.113	1.040	1.082	0.967
final R indices [$I > 2\sigma(I)$]	R_1 = 0.0464, wR_2 = 0.1099	R_1 = 0.0275 wR_2 0.0696	R_1 = 0.0303 wR_2 = 0.0749	R_1 = 0.0460 wR_2 = 0.1127
R indices (all data)	R_1 = 0.0839, wR_2 = 0.1442	R_1 = 0.0390, wR_2 = 0.0776	R_1 = 0.0529, wR_2 = 0.0946	R_1 = 0.0959, wR_2 = 0.1367
largest diff peak/hole [e Å^{-3}]	1.297 and −1.764	1.401 and −1.280	0.907/−1.757	1.926 and −1.534

[a] Data common to all structures: temp of collection, 173(2) K; λ, 0.71073 Å; refinement method, full-matrix least-squares on F^2; Bruker-AXS Smart 1000 diffractometer.

Table 3. Key Interatomic Distances (Å) and Angles (deg) for Diplatinum Complexes

	8[a]	**9**·CH_2Cl_2[a]	**17**
Pt1···Pt2	7.742 (6)	7.759	10.3628 (3)
sum of all bond lengths from Pt1 to Pt2	7.833	7.830	10.293
Pt1−C1	2.009 (11)	1.988 (4)	1.995 (5)
C1≡C2	1.202 (14)	1.225 (5)	1.119 (6)
C2−C3	1.400 (14)	1.373 (5)	1.367 (6)
C3≡C4	1.196 (13)	1.221 (5)	1.215 (7)
C4−C5			1.373 (7)
C5≡C6			1.216 (6)
C4(C6)−Pt2	2.026 (9)	2.024 (3)	2.008 (5)
Pt1−C11$_{ipso}$	2.081 (11)	2.078 (4)	2.055 (5)
Pt2−C21$_{ipso}$	2.075 (9)	2.059 (3)	2.062 (5)
Pt1−P1	2.300 (3)	2.2899 (10)	2.2998 (11)
Pt1−P2	2.291 (3)	2.2987 (8)	2.2907 (11)
Pt2−P3	2.295 (3)	2.2850 (8)	2.2864 (11)
Pt2−P4	2.287 (2)	2.2976 (9)	2.2986 (12)
Pt1−C1−C2	172.5 (8)	173.2 (3)	176.9 (4)
C1−C2−C3	173.8 (10)	177.4 (4)	178.0 (5)
C2−C3−C4	175.6 (11)	176.1 (4)	178.5 (5)
C3−C4−C5			178.7 (6)
C4−C5−C6			179.3 (5)
C3(C5)−C4(C6)−Pt2	174.1 (9)	171.2 (3)	176.8 (4)
P−Pt−P/Pt angle[b]	62.3	35.1	1.5
Pt−P−P−C$_{ipso}$−C1 angle[b]	60.1	34.7	5.1

[a] The atomic numbering sequence C11−Pt1−C1−C2−C3−C4−Pt2−C21 has been reversed from that in the CIF file to facilitate comparisons with the other complexes. [b] Angle between the planes defined by these atoms on each end-group.

Table 4. Key Interatomic Distances (Å) and Angles (deg) for 18·$(C_7H_8)_{0.5}$

	molecule 1	molecule 2
Pt1···Au	7.787	7.788
sum of all bond lengths from Pt to Au	7.792	7.794
Pt1−C1	2.003 (11)	1.988 (10)
C1≡C2	1.213 (13)	1.221 (13)
C2−C3	1.368 (15)	1.356 (15)
C3≡C4	1.218 (13)	1.222 (13)
C4−Au	1.990 (10)	2.007 (11)
Pt−C11$_{ipso}$	2.107 (10)	2.081 (9)
Pt1−P1	2.304 (2)	2.301 (2)
Pt1−P2	2.302 (2)	2.307 (2)
Au−P3	2.272 (3)	2.279 (3)
Pt1−C1−C2	177.3 (9)	177.2 (8)
C1−C2−C3	178.5 (11)	179.5 (11)
C2−C3−C4	178.1 (11)	178.0 (11)
C3−C4−Au	178.5 (9)	176.4 (9)
C4−Au−P3	176.7 (2)	177.1 (2)

to longer wavelengths than the platinum/gold complex **18**. This feature suggested a greater degree of π-delocalization in the former. Complex **18** also exhibited a very intense UV transition at 280 nm. Given the absence of a counterpart in **9**, this was presumed to be associated with the Ph_3PAuC_4 moiety.

At room temperature, neither **9** or **18** exhibited emission. However, at low temperature in a MTHF glass, both complexes showed a bright and highly structured emission (Figures 5b and 5d). The emission was assigned to phosphorescence from a triplet state concentrated on the butadiynediyl segments. This is supported by the lifetimes, which were ca. 6.5 and 15 μs for **9** and **18**, respectively. The emission spectra for both complexes appeared as a manifold of narrow vibronic sub-bands separated by approximately 2200 cm^{-1}. This progression was attributed to the stretching mode of the butadiynediyl chains. Utilizing methods described in previous papers,[9,28] the phosphorescence spectra for **9** and **18** at 80 K were analyzed by a single-mode Franck−Condon expression,

$$I(\bar{\nu}) = \sum_{\nu_m=0}^{5} \left\{ \left(\frac{E_{00} - \nu_m \hbar\omega_m}{E_{00}} \right)^3 \frac{(S_m)^{\nu_m}}{\nu_m!} \times \exp\left[-4 \ln 2 \left(\frac{\bar{\nu} - E_{00} + \nu_m \hbar\omega_m}{\Delta\bar{\nu}_{0,1/2}} \right)^2 \right] \right\} \quad (1)$$

where $I(\nu)$ is the relative emission intensity at energy ν, E_{00} is the energy of the 0−0 transition, ν_m is the quantum number of the

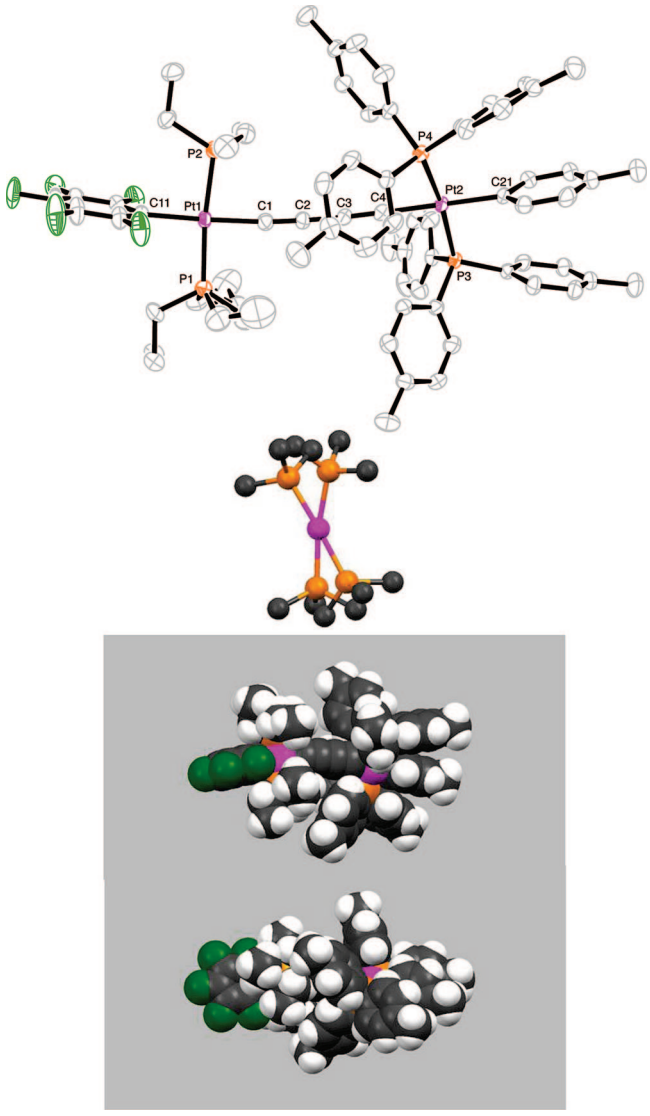

Figure 2. Thermal ellipsoid (top; 50% probability level), Newman (middle), and space-filling (bottom) representations of **9**.

average medium-frequency vibrational mode, $\hbar\omega_m$ is the average medium-frequency acceptor modes coupled to the triplet-excited-state to ground-state transition, S_m is the Huang−Rhys factor, and $\Delta\nu_{0,1/2}$ is the half-width of the individual vibronic bands. The experimental emission spectra were fitted using a macro in Microsoft Excel.[9] A summary of the parameters recovered from the fits is provided in Table 5.

Several interesting features emerge from Table 5. First, the 0−0 emission energy for the PtC_4Au complex **18** is ca. 900 cm^{-1} higher than that for the PtC_4Pt' complex **9**. Second, the Huang−Rhys parameter (S_m) is noticeably smaller for the latter. Both of these features are consistent with the notion that the triplet wave function is spatially more concentrated in the platinum/gold system. Excitation spectra were recorded while monitoring the 0−0 emission band (80 K), as depicted as overlays with the absorption spectra in Figures 5a and 5c. The excitation spectra reflect the absorption spectra, except that the vibronic structure is better resolved. This is likely due to the frozen glass matrix.

(28) Whittle, C. E.; Weinstein, J. A.; George, M. W.; Schanze, K. S. *Inorg. Chem.* **2001**, *40*, 4053.

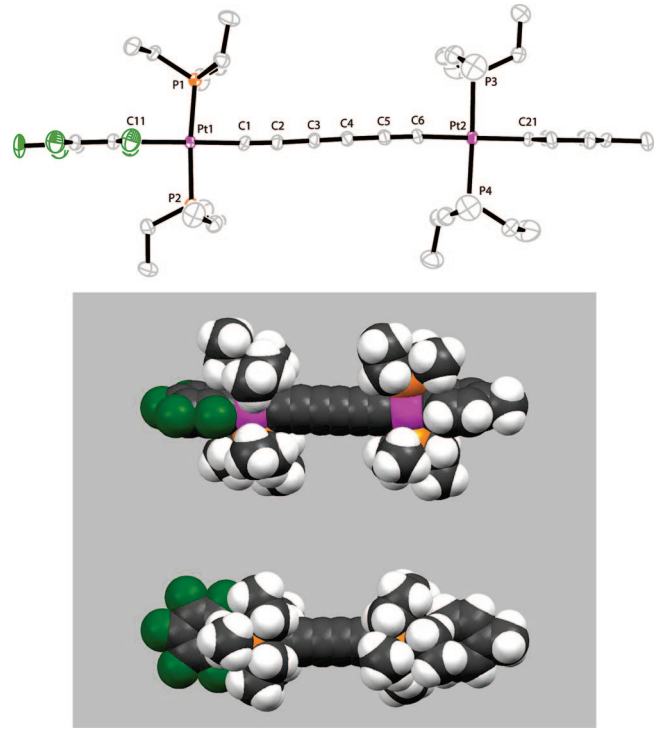

Figure 3. Thermal ellipsoid (top; 50% probability level) and space-filling (bottom) representations of **17**.

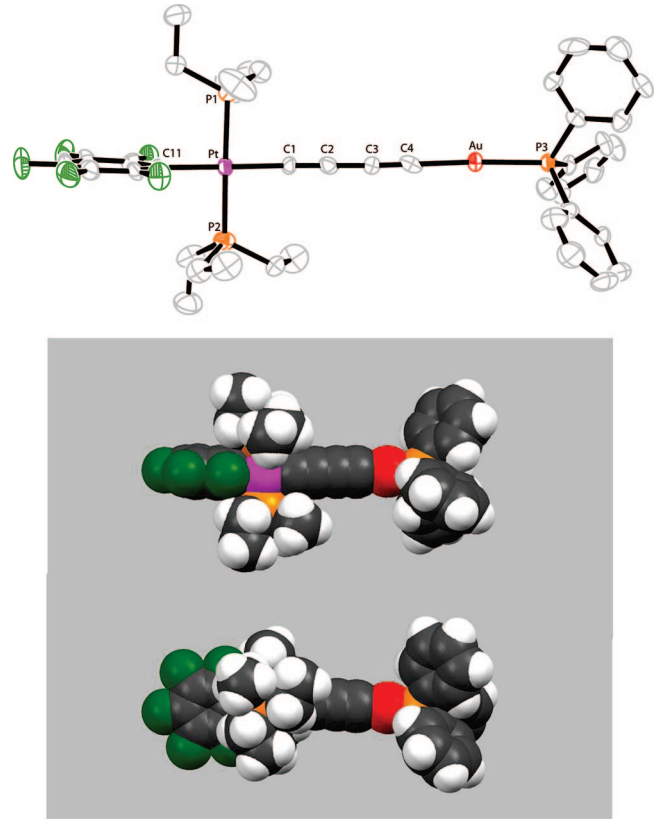

Figure 4. Thermal ellipsoid (top; 50% probability level) and space-filling (bottom) representations of **18**.

The emission spectra were next studied as a function of temperature from 80 K to room temperature. For **18**, the spectra were unaffected by increasing temperature and only the intensity decreased. However, an interesting feature emerged with **9**. At 80 K in the frozen glass, the spectrum

Table 5. Emission Spectral Fitting Parameters for the PtC_4Pt' and PtC_4Au Complexes 9 and 18 at 80 K

complex	λ_{abs}/nm (ε/M^{-1} cm^{-1})[a]	λ_{max}, em	E_{00}/cm^{-1}	$\hbar\omega$/cm^{-1}	$\Delta\nu_{0.1/2}$/cm^{-1}	S_m	τ/μs
9	279 (25000) 326 (14000) 352 (13000)	432	23 150	2184	480	0.78	6.49 ± 0.10
18	280 (55000) 297 (52000) 325 (14000)	416	24 035	2158	335	1.03	14.9 ± 1.85

[a] Recorded in 2-methyltetrahydrofuran (MTHF) at room temperature.

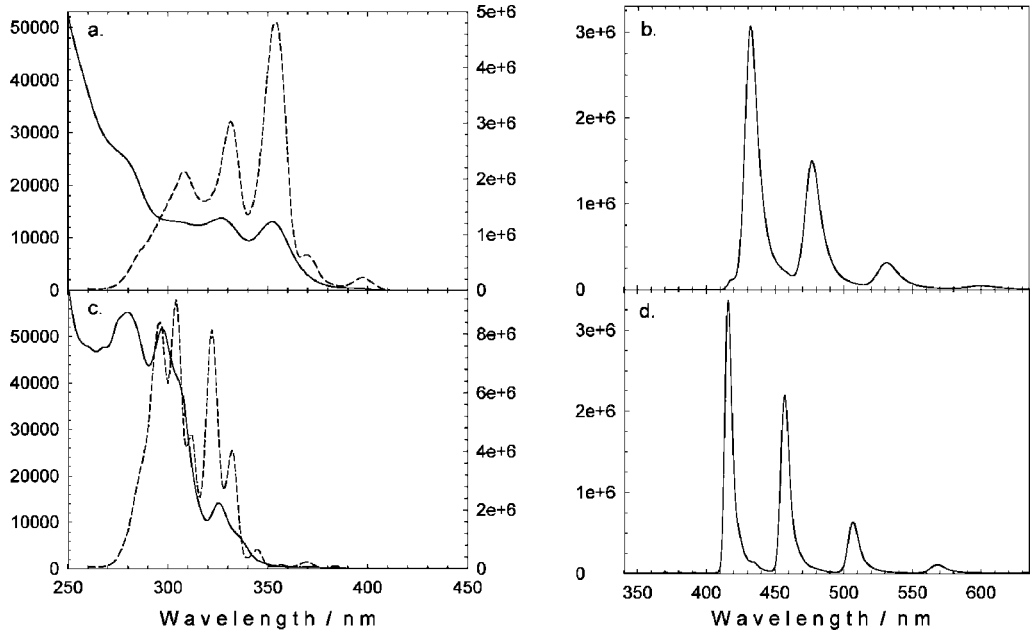

Figure 5. (a) Absorption (solid line; room temperature) and excitation (dashed line, 81 K, λ_{em} = 418 nm) spectra of **9** in MTHF (2-methyltetrahydrofuran). (b) Emission spectrum of **9** (81 K, λ_{ex} = 352 nm). (c) Absorption (solid line; room temperature) and excitation (dashed line, 81 K, λ_{em} = 416 nm) spectra of **18** in MTHF. (d) Emission spectrum of **18** (81 K, λ_{ex} = 325 nm).

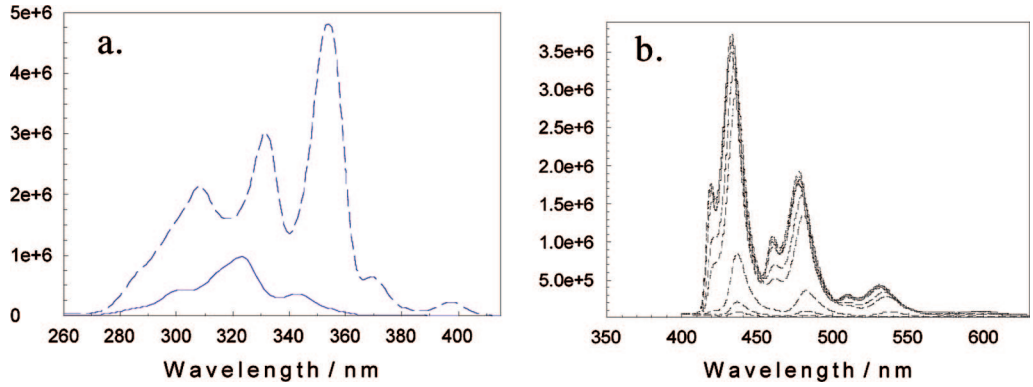

Figure 6. (a) Excitation spectra of **9** (81 K, MTHF), λ_{em} = 418 nm (dashed line) and λ_{em} = 432 nm (solid line). (b) Variable-temperature emission spectra of **9** (λ_{ex} = 326 nm) in order of decreasing intensity: 80, 88, 91, 96, 102, 107, 110, 117, 121, 125 K.

varied with excitation wavelength. The spectrum shown in Figure 5b was obtained with 352 nm excitation, coincident with the maximum in the excitation spectrum in Figure 5a. A substantially different spectrum was observed when the 80 K sample was excited at shorter wavelength (e.g., 326 nm, Figure 6b). In this case, the emission showed two distinct vibronic progressions, suggesting the existence of heterogeneity. Figure 6a compares the emission excitation spectra of **9** obtained at the peaks of the two 0−0 bands in the emission spectra. It can easily be seen that the higher energy emission has an excitation profile that is blue-shifted compared to that of the more intense, lower energy emission. Finally, and especially noteworthy, upon warming the sample above the solvent glass−fluid transition temperature (120 K), the high energy progression disappeared, and the emission was dominated only by the single 0−0 band and vibronic progression characteristic of the diplatinum complex. A rationale for these observations involving two distinct triplet conformers is proposed below.

Discussion

1. Syntheses of Title Complexes. As summarized in Scheme 1 (bottom), prior to this study we had been able to prepare two

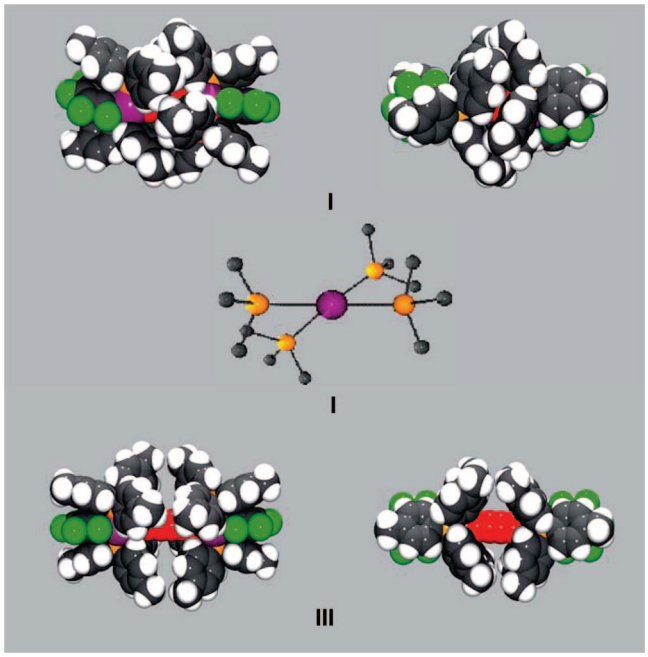

Figure 7. Space-filling representations of **I** and **III** (top and bottom) and a Newman projection of **I** (middle).

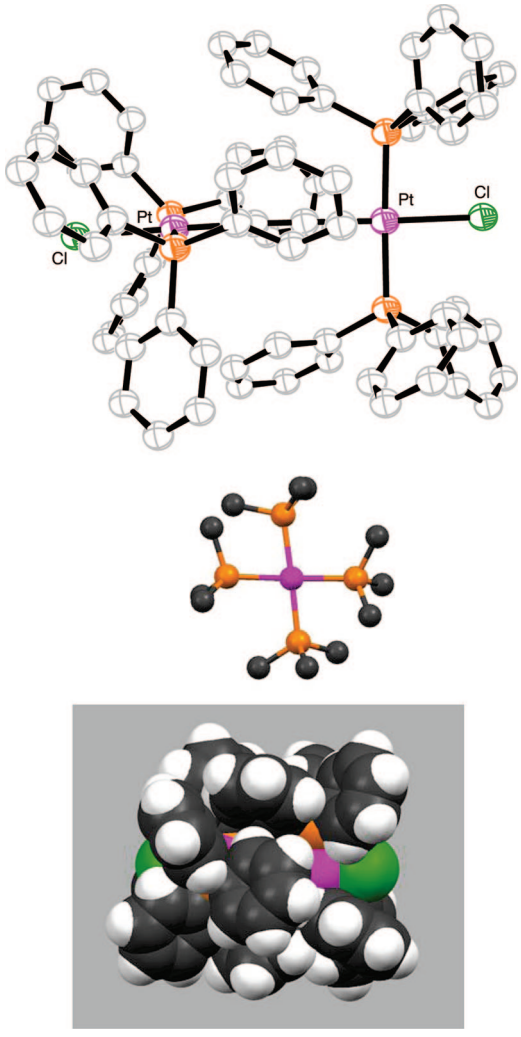

Figure 8. Thermal ellipsoid (top; 50% probability level), Newman (middle), and space-filling (bottom) representations of *trans*,*trans*-$Cl(Ph_3P)_2PtC{\equiv}CPt(PPh_3)_2Cl$.

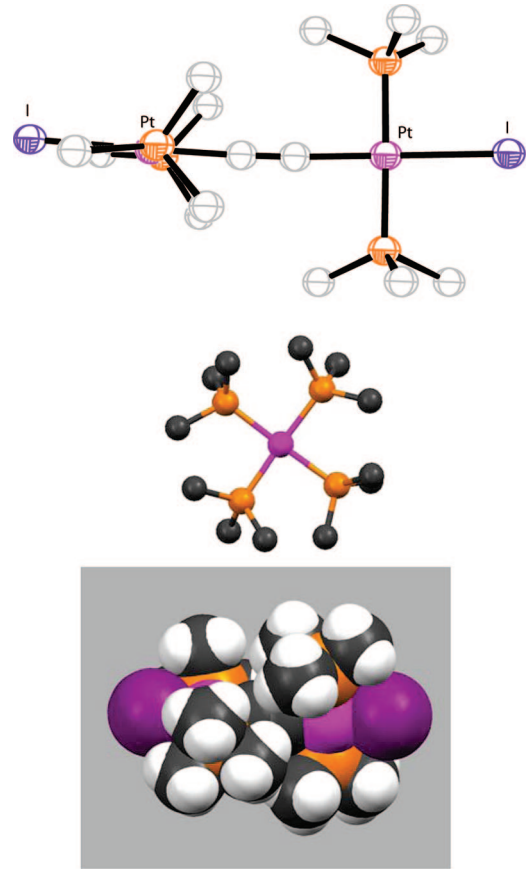

Figure 9. Thermal ellipsoid (top; 50% probability level), Newman (middle), and space-filling (bottom) representations of *trans*,*trans*-$I(Me_3P)_2PtC{\equiv}CPt(PMe_3)_2I$.

symmetrically substituted butadiynediyl complexes by Hagihara heterocouplings, C_6F_5/*p*-tol_3P-substituted **I**[2] and C_6F_5/Et_3P-substituted **II**,[7] as well as analogous C_6F_5/*p*-tol_3P- and *p*-tol/*p*-tol_3P-substituted hexatriynediyl (**III**, **IV**) and *p*-tol/*p*-tol_3P-substituted decapentaynediyl (**V**) complexes.[2,3] These results, together with the successful and unsuccessful syntheses of unsymmetrically substituted homologues in Schemes 2−4 and related data, suggest that steric and electronic factors play key roles in these couplings. For example, note that as the lengths of the polyynyl ligands in Scheme 1 (bottom) increase, lower temperatures can be employed. Progressively lower temperatures also suffice for the homocouplings in Scheme 1 (top).[2,3] The Brønsted acidities of terminal polyynes, which may be of mechanistic relevance, are known to increase with the sp chain length.[29]

Scheme 2 shows that despite the successful synthesis of **I**, all attempts to prepare a homologue in which one pentafluorophenyl ligand has been replaced by *p*-tolyl have been unsuccessful. For reference, a space-filling representation of the crystal structure of **I**[6d] is shown in Figure 7 (top). This dramatically illustrates the steric interactions between the end-groups, which intimately embrace. In contrast, there are no end-group/end-group steric interactions in the homologous hexatriynediyl complex **III** (Figure 7, bottom).[6d] The hexatriynediyl complex with PEt_3 ligands has also been structurally characterized, and the van der Waals separation of the end-groups is even greater.[6d]

Accordingly, Scheme 2 shows that unsymmetrically substituted butadiynediyl complexes are easily accessed when the *p*-tol_3P ligands on one or both end-groups are replaced by Et_3P ligands. As would be intuitively expected from the

results in Scheme 1 (bottom), Scheme 4 establishes that unsymmetrically substituted hexatriynediyl complexes can be prepared with either *p*-tol$_3$P or Et$_3$P ligands. However, we do not presently have a rationale for our inability to cross-couple **11** and **4** (Scheme 4, bottom). In principle, certain complexes might be accessed by alternative combinations of coupling partners (e.g., *trans*-(*p*-tol)(R$_3$P)$_2$Pt(C≡C)$_2$H and *trans*-(C$_6$F$_5$)(Et$_3$P)$_2$PtCl for **8** and **9** (Scheme 3)), but such details were beyond the scope of this initial exploratory study.

We have also prepared an unsymmetrically substituted octatetraynediyl complex by the displacement of one chloride ligand in *trans*,*trans*-Cl(*p*-tol$_3$P)$_2$Pt(C≡C)$_4$Pt(P*p*-tol$_3$)$_2$Cl.[5] However, it is difficult to avoid disubstitution in such desymmetrizations, and we consider such strategies intrinsically less general. Numerous other symmetrically substituted diplatinum butadiynediyl, hexatriynediyl, and ethynediyl complexes have been synthesized.[30] Tellingly, all butadiynediyl and ethynediyl complexes prepared by Hagihara-type couplings have been limited to tri(*n*-alkyl)phosphine-containing end-groups.[18] Hagihara couplings will also likely be limited by the stabilities of the precursor polyynyl complexes L$_y$Pt(C≡C)$_n$H, which decrease dramatically as the sp chain is lengthened.[2,3] However, under carefully controlled conditions, Hay homocouplings have been effected with tetradecaheptaynyl complexes (n = 7).[3]

2. Structural and Electrochemical Data. Curiously, nearly all symmetrically substituted diplatinum polyynediyl complexes with C$_6$ or longer chains crystallize with nearly coplanar end-groups (±18.4°).[2−6] Since DFT calculations do not indicate any electronic conformational preference in the singlet ground state,[27] this is presumed to reflect a deep-seated crystal lattice effect. Accordingly, the end-group/end-group angle in the hexatriynediyl complex **17** is close to 0° (5.1−1.5°), exactly as in the symmetrically substituted homologues with *trans*-(*p*-tol)(Et$_3$P)$_2$Pt and *trans*-(*p*-tol)(*p*-tol$_3$P)$_2$Pt end-groups.[6d] However, analogously to the situation with biaryls Ar(C≡C)$_n$Ar (n = 0−2),[31] coplanar end-groups become impossible when the C$_x$ bridges are too short or the end-group substituents too large.

Thus, the end-group/end-group angle in the *p*-tol$_3$P-substituted butadiynediyl complex **I** (Figure 7) increases to 41.0−40.8°. That in Et$_3$P-substituted butadiynediyl complex **8** (Figure 1) is 62.3−60.1°. Curiously, that in the mixed *p*-tol$_3$P/Et$_3$P complex **9** (Figure 2) is lowest, 35.1−34.7°. The crystal structures of two ethynediyl complexes, *trans*,*trans*-X(R$_3$P)$_2$PtC≡CPt(PR$_3$)$_2$X (X/R = Cl/Ph, I/Me), are depicted in Figures 8 and 9.[18b,30a] The end-group/end-group angles in these much more congested systems increase to 82−90°, maximizing the separation of phosphine ligands on opposite termini. In the Ph$_3$P complex, the C$_2$ chain is completely shielded. This species was isolated in an impressive 94% yield from a reaction of the chloroethynyl complex *trans*-Cl(Ph$_3$P)$_2$PtC≡CCl and the ethylene adduct of Pt(PPh$_3$)$_2$, a method that would not be applicable to the title complexes.

Despite the low coordination number of the gold atom in **18**, there are no close contacts in the crystal, in accord with most other triarylphosphine gold alkynyl complexes.[32] The nearest gold/gold distance (7.47 Å) is outside of the range associated with aurophilic interactions, which normally require smaller trialkylphosphine ligands to be observed in gold alkynyl complexes.[32] Interestingly, pairs of molecules pack in a head-to-head manner, such that Ph$_3$P ligands exhibit a sextuple phenyl embrace.[33] The corresponding phosphorus−phosphorus and gold−gold distances are 7.47 and 11.56 Å, respectively.

As summarized in Table 1, the diplatinum complexes give partially reversible oxidations that are presumed to generate mixed valence radical cations.[34] The oxidations of the butadiynediyl complexes **8** and **9** are thermodynamically more favorable (less positive ΔE) and exhibit a larger degree of reversibility (higher $i_{c/a}$) than the hexatriynediyl complexes **12** and **17**. Analogous chain length effects are observed with the symmetrically substituted complexes (e.g., **I** vs **III**)[2,3] and follow logically from the HOMO energies.[27] Complex **8**, which can be derived from **II** by replacing one electron-withdrawing pentafluorophenyl ligand by an electron-releasing *p*-tolyl ligand, is as expected more easily oxidized. Complex **12**, which has an analogous relationship to **III**, is also more easily oxidized. However, as illustrated by **IV** and its higher homologues,[3] *p*-tolyl ligands can have a deleterious affect upon reversibility. It has been suggested that the pentafluorophenyl moiety may in some way hinder a subsequent chemical reaction that involves the aryl substituent.[3] The platinum/gold complex **18** also gives only irreversible oxidations, perhaps in part due to the decreased steric shielding of the C$_4$ chain.

3. Photophysical Data. The PtC$_4$Pt′ and PtC$_4$Au complexes **9** and **18** exhibit highly structured phosphorescence emissions at 80 K in rigid MTHF glasses. The triplet states responsible for these emissions are concentrated on the C$_4$ units, as evidenced by the dominant vibrational progression due to the C≡C stretching mode. Nevertheless, several features suggest that the triplet wave function is delocalized into the platinum atom via π(C)−dπ(Pt) orbital overlap, but not to any significant extent into the gold atom in **18**. First, the 0−0 emission energy of **9** appears at a lower energy than that of **18**. This may be due to the influence of the two platinum end-groups in **9** compared to only one in **18**. Second, the Huang−Rhys constant, which provides a relative measure of the degree of excited state delocalization, is smaller for **9** compared to **18**. This also suggests a greater degree of triplet state delocalization in the diplatinum complex. It is further significant that, in an earlier study, Che and co-workers reported the phosphorescence of the digold complex Cy$_3$PAu(C≡C)$_2$AuPCy$_3$, which showed an emission with the same 0−0 energy as **18**.[35] However, inspection of the spectrum of Cy$_3$PAu(C≡C)$_2$AuPCy$_3$ suggests that the Huang−Rhys constant is larger than that of **18**, consistent with some delocalization of the triplet wave function into the platinum center in the latter complex.

(29) Eastmond, R.; Johnson, T. R.; Walton, D. R. M. *J. Organomet. Chem.* **1973**, *50*, 87.

(30) For additional Pt(C≡C)$_n$Pt complexes (n = 1−3), see ref 18b and (a) Sünkel, K.; Birk, U.; Robl, C. *Organometallics* **1994**, *13*, 1879. (b) Klein, A.; Klinkhammer, K.-W.; Scheiring, T. *J. Organomet. Chem.* **1999**, *592*, 128. (c) Müller, C.; Lachicotte, R. J.; Jones, W. D. *Organometallics* **2002**, *21*, 1190. (d) Wong, W.-Y.; Wong, C.-K.; Lu, G.-L.; Cheah, K.-W.; Shi, J.-X.; Lin, Z. *J. Chem. Soc., Dalton Trans.* **2002**, 4587. (e) Yam, V. W.-W.; Wong, K. M.-C.; Zhu, N. *Angew. Chem., Int. Ed* **2003**, *42*, 1400; *Angew. Chem.* **2003**, *115*, 1438.

(31) (a) Brizius, G.; Billingsley, K.; Smith, M. D.; Bunz, U. H. F. *Org. Lett.* **2003**, *5*, 3951. (b) Toyota, S.; Iida, T.; Kunizane, C.; Tanifuji, N.; Yoshida, Y. *Org. Biomol. Chem.* **2003**, *1*, 2298. (c) Makino, T.; Toyota, S. *Bull. Chem. Soc. Jpn.* **2005**, *78*, 917. (d) Toyota, S.; Yanagihara, T.; Yoshida, Y.; Goichi, M. *Bull. Chem. Soc. Jpn.* **2005**, *78*, 1351. (e) Miljaniæ, O. S.; Han, S.; Holmes, D.; Schaller, G. R.; Vollhardt, K. P. C. *Chem. Commun.* **2005**, 2606. (f) Nandy, R.; Subramoni, M.; Varghese, B.; Sankararaman, S. *J. Org. Chem.* **2007**, *72*, 938.

(32) Liau, R.-Y.; Schier, A.; Schmidbaur, H. *Organometallics* **2003**, *22*, 3199.

(33) (a) Scudder, M.; Dance, I. *Chem.−Eur. J.* **2002**, *8*, 5456. (b) Dance, I.; Scudder, M. *New J. Chem.* **1998**, 481.

(34) For other mixed valence diplatinum radical cations, see: Klein, A.; Kaim, W. *Organometallics* **1995**, *14*, 1176.

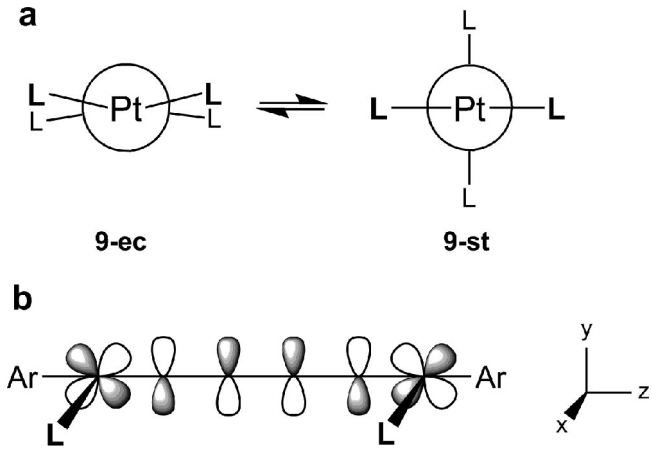

Figure 10. (a) Eclipsed (**9-ec**) and staggered (**9-st**) conformations of the triplet excited state of diplatinum complex **9**. (b) Schematic of interactions between the symmetric combination of d_{yz} orbitals on the platinum atoms and the symmetric π_y* orbital of the C_4 chain in **9-ec**.

As noted above, the emission of **9** in the frozen solvent glass features two distinct 0−0 bands and corresponding vibrational progressions, suggesting the presence of sample (or site) heterogeneity in the glass. The heterogeneity disappears above the solvent glass-to-fluid transition. This behavior is not observed with **18**, suggesting that two platinum end-groups are necessary for heterogeneity. In previous studies, we and others have used density functional calculations to explore the nature of the dπ(Pt)−pπ(C) interactions in platinum polyynyl and diplatinum polyynediyl complexes.[27,36] The data clearly indicate that the relative orientation of the square-planar end-group relative to the π-electron system of the C_x chain affects the energy of the relaxed triplet excited state.

We suggest that the spectroscopic heterogeneity observed for triplet **9** in the low-temperature glass arises from noninterconverting conformers with roughly eclipsed and staggered geometries (**9-ec** and **9-st**, Figure 10a). The latter represents an excited state analogue of the sterically mandated conformations of the ethynediyl complexes in Figures 8 and 9. The heterogeneity disappears above the solvent glass-to-fluid transition due to relaxation to the lower energy conformation. Note that the end-group/end-group angle in crystalline singlet **9** (35.1−34.7°) is closer to that of **9-ec**.

The spectroscopic heterogeneity would be rationalized by different degrees of triplet excited state delocalization in **9-ec** and **9-st**. That in the former should be greater due to the uninterrupted conjugation between both platinum atoms and the π-system of the C_4 chain. For example, as shown in Figure 10b, an unfilled π_y* level of the C_4 chain can interact with the filled d_{xy} levels on each platinum center, leading to two filled MOs that are delocalized across the entire PtC_4Pt system. A similar, fully delocalized array cannot exist in **9-st** since the dπ orbital systems on the two platinum end-groups are orthogonal. This is furthermore consistent with the absence of spectroscopic heterogeneity with the PtC_4Au complex **18**, which is incapable of conformational isomerism due to the effective cylindrical symmetry of the gold end-group.

4. Conclusion

This study has established methodology for accessing unsymmetrically substituted butadiynediyl and hexatriynediyl complexes containing one and two platinum end-groups. Although some limitations due to steric and electronic effects are evident, successful extensions to higher homologues can be anticipated, up to the point where the $Pt(C{\equiv}C)_nH$ coupling partners become too unstable. It also probable that the very stable platinum/gold complex **18**, and analogues thereof, will constitute useful building blocks for preparing species with longer sp carbon chains. With the butadiynediyl complexes, both structural and low-temperature phosphorescence data underscore the important influence that end-group/end-group interactions can have upon molecular properties at short C_x chain lengths. Efforts are currently underway to exploit such interactions to generate new classes of atropisomers.[37]

Experimental Section

1. General Procedures. General procedures, chemical sources and purifications, instrumentation, and protocols for the photophysical studies were identical with those in three previous papers.[6b,c,9] The one chemical new to this study outside of those with literature citations below ($KN(SiMe_3)_2$, Fluka; 0.5 M in toluene) was used as received.

***trans,trans*-$(C_6F_5)(Et_3P)_2Pt(C{\equiv}C)_2Pt(PEt_3)_2$(*p*-tol) (8).** A Schlenk flask was charged with *trans*-$(C_6F_5)(Et_3P)_2Pt(C{\equiv}C)_2H$ (**6**;[7] 0.058 g, 0.090 mmol), *trans*-(*p*-tol)$(Et_3P)_2PtCl$ (**7**;[7] 0.050 g, 0.090 mmol), CuCl (0.0020 g, 0.020 mmol), and $HNEt_2$ (6 mL) with stirring. After 120 h, the solvent was removed by oil pump vacuum. The residue was chromatographed (two successive silica gel columns: 20 × 1 cm, 60:40 v/v hexanes/CH_2Cl_2; 15 × 1 cm, 50:50 v/v hexanes/toluene). The solvent was removed from the product-containing fractions by oil pump vacuum. The yellow residue was washed with ethanol (1 mL) to give **8** as an off-white powder (0.065 g, 0.056 mmol; 62%), mp 112 °C. Anal. Calcd for $C_{41}H_{67}F_5P_4Pt_2$: C, 42.12; H, 5.78. Found: C, 41.76; H, 5.74. DSC:[34] endotherm with T_i, 84.8 °C; T_e, 110.5 °C; T_c, 113.3 °C; T_f, 138.9 °C. TGA: weight loss 58%, 220−414 °C. NMR (δ, $CDCl_3$): ^{1}H 7.13 (d, 2H, $^3J_{HH}$ = 7.7 Hz, $^3J_{HPt}$ = 38 Hz,[39] *o* to Pt), 6.75 (d, 2H, $^3J_{HH}$ = 7.7 Hz, *m* to Pt), 2.17 (s, 3H, CH_3 *p* to Pt), 1.79−1.73 (m, 12H, PCH_2), 1.72−1.69 (m, 12H, P′CH_2), 1.07−0.99 (m, 36H, PCH_2CH_3/P′CH_2CH_3); $^{13}C\{^1H\}$[40] 151.2 (s, *i* to Pt), 138.8 (s, *o* to Pt), 129.9 (s, *p* to Pt), 128.1 (s, $^3J_{CPt}$ = 23.5 Hz,[39] *m* to Pt), 97.8 (s, PtC≡), 97.4 (s, PtC≡*C*), 95.5 (s, PtC≡*C*), 29.7 (s, CH_3 *p* to Pt), 15.6 (virtual t, $^1J_{CP}$ = 17.4 Hz,[41] PCH_2), 15.1 (virtual t, $^1J_{CP}$ = 17.2 Hz,[41] P′CH_2), 8.0 (s, PCH_2CH_3), 7.8 (s, P′CH_2CH_3); $^{31}P\{^1H\}$ 13.1 (s, $^1J_{PPt}$ = 2459 Hz, P_{C6F5}),[39] 10.3 (s, $^1J_{PPt}$ = 2649 Hz, $P_{p\text{-}tol}$).[39] IR (cm^{-1}, powder film): $\nu_{C\equiv C}$ not observed. UV−vis (CH_2Cl_2, 1.25 × 10^{-5} M):[42] 318 (16700), 338 (18700). MS:[43] 1168 (M^+, 100%), 1077 ($[M - tol)]^+$, 10%), 765 ($[M - C_6F_5 - 2PEt_3]^+$, 50%), 597 ($[(C_6F_5)(Et_3P)_2Pt]^+$, 20%), 522 ($[(tol)(Et_3P)_2Pt]^+$, 100%).

(35) Che, C.-M.; Chao, H.-Y.; Miskowski, V. M.; Li, Y.; Cheung, K.-K. *J. Am. Chem. Soc.* **2001**, *123*, 4985.

(36) (a) Glusac, K.; Kose, M. E.; Jiang, H.; Schanze, K. S. *J. Phys. Chem. B* **2007**, *111*, 929. (b) Cooper, T. M.; Blaudeau, J.-P.; Hall, B. C.; Rogers, J. E.; McLean, D. G.; Liu, Y.; Toscano, J. P. *Chem. Phys. Lett.* **2004**, *400*, 239.

(37) Dey, S. Work in progress, Texas A&M University.

(38) DSC and TGA data were treated as recommended by: Cammenga, H. K.; Epple, M. *Angew. Chem., Int. Ed. Engl.* **1995**, *34*, 1171; *Angew. Chem.* **1995**, *107*, 1284. The T_e values best represent the temperature of the phase transition or exotherm.

(39) This coupling represents a satellite (d; ^{195}Pt = 33.8%) and is not reflected in the peak multiplicity given.

(40) Unless otherwise noted, one PtC and the C_6F_5 ^{13}C NMR signals were not observed. The PtC_xPt signals were assigned according to chemical shift and coupling constant trends established for closely related species.[2,3,6d,7]

(41) Hersh, W. H. *J. Chem. Educ.* **1997**, *74*, 1485; the $^nJ_{CP}$ values represent the *apparent* couplings between adjacent peaks of the triplet.

***trans,trans*-(C_6F_5)(Et_3P)$_2$Pt(C≡C)$_2$Pt(P*p*-tol$_3$)$_2$(*p*-tol) (9).** A Schlenk flask was charged with **6** (0.162 g, 0.250 mmol), *trans*-(*p*-tol)(*p*-tol$_3$P)$_2$PtCl (**4**;[3] 0.233 g, 0.250 mmol), *t*-BuOK (0.0338 g, 0.301 mmol), KPF_6 (0.0561 g, 0.304 mmol), CuCl (0.0049 g, 0.049 mmol), THF (10 mL), and methanol (10 mL) with stirring. After 96 h, the solvent was removed by oil pump vacuum. The residue was extracted with CH_2Cl_2. The extract was filtered through a short alumina/Celite pad. The solvent was removed by rotary evaporation and oil pump vacuum to give **9** as a pale yellow solid (0.350 g, 0.228 mmol; 91%), dec pt > 167 °C (gradual darkening, then melting). Anal. Calcd for $C_{71}H_{79}F_5P_4Pt_2$: C, 55.32; H, 5.17. Found: C, 55.33; H, 5.17. DSC:[38] endotherm with T_i, 105.3 °C; T_e, 108.9 °C; T_c, 122.0 °C; T_f, 122.2 °C; exotherm with T_i 122.2 °C; T_e, 122.2 °C; T_c, 132.0 °C; T_f, 132.1 °C; endotherm with T_i, 132.2 °C; T_e, 132.2 °C; T_c, 143.5 °C; T_f, 144.5 °C; endotherm with T_i, 163.8 °C; T_e, 179.6 °C; T_c, 187.6 °C; T_f, 191.2 °C. TGA: weight loss 36%, 195−403 °C. NMR (δ, $CDCl_3$): ^{1}H 7.43−7.39 (m, 12H, *o* to P), 6.98 (d, 12H, $^3J_{HH}$ = 7.7 Hz, *m* to P), 6.29 (d, 2H, $^3J_{HH}$ = 7.7 Hz, *o* to Pt), 5.98 (d, 2H, $^3J_{HH}$ = 7.5 Hz, *m* to Pt), 2.29 (s, 18H, CH_3 *p* to P), 1.90 (s, 3H, CH_3 *p* to Pt), 1.54−1.51 (m, 12H, PCH_2), 0.95−0.89 (m, 18H, PCH_2CH_3); ^{13}C{^{1}H}[40] 152.2 (s, *i* to Pt), 139.2 (s, *o* to Pt), 139.1 (s, *p* to P), 134.6 (s, *o* to P), 128.9 (virtual t, $^1J_{CP}$ = 29.0 Hz,[41] *i* to P), 128.6 (s, *p* to Pt), 128.0 (s, *m* to P), 127.4 (s, *m* to Pt), 103.1 (s, PtC≡), 99.4 (s, PtC≡*C*), 96.0 (s, PtC≡*C*), 21.4 (s, CH_3 *p* to P), 20.5 (s, CH_3 *p* to Pt), 15.5 (virtual t, $^1J_{CP}$ = 17.5 Hz,[41] PCH_2), 7.8 (s, PCH_2CH_3); ^{31}P{^{1}H} 18.3 (s, $^1J_{PPt}$ = 2987 Hz, P*p*-tol$_3$),[39] 12.9 (s, $^1J_{PPt}$ = 2461 Hz, PEt_3).[39] IR (cm^{-1}, powder film), $\nu_{C\equiv C}$ 2148 (w), 2001 (w); UV−vis (CH_2Cl_2, 1.25 × 10^{-5} M; MTHF, see Table 5 and Figure 5),[42] 300 (15 400), 324 (13800), 349 (13 300). MS:[43] 1541 (M^+, 90%), 1449 ([M − tol]$^+$, 30%), 1358 ([M − C_6F_5]$^+$, 3%), 950 ([M − C_6F_5 − PEt_3 − P*t*ol$_3$]$^+$, 100%).

***trans,trans*-(C_6F_5)(*p*-tol$_3$P)$_2$Pt(C≡C)$_3$Pt(P*p*-tol$_3$)$_2$(*p*-tol) (12). A.** A Schlenk flask was charged with **4** (0.0484 g, 0.0520 mmol), $HNEt_2$ (20 mL), and CuCl (0.0040 g, 0.040 mmol) with stirring and cooled to −45 °C. Another Schlenk flask was charged with *trans*-(C_6F_5)(*p*-tol$_3$P)$_2$Pt(C≡C)$_3$SiEt_3 (**13**,[3] 0.0600 g, 0.0520 mmol) and CH_2Cl_2 (2 mL), and *n*-$Bu_4N^+F^-$ (0.016 mL, 1.0 M in THF, 5 wt % H_2O) was added with stirring. After 15 min, the solution derived from **13** was added via syringe to that of **4**. The mixture was allowed to warm at room temperature overnight. After 6 days, the solvent was removed by oil pump vacuum. The residue was extracted with hexanes (3 × 5 mL) and toluene (3 × 7 mL). The extracts were passed in sequence through an alumina column (4 × 1 cm), which was rinsed with toluene. The solvent was removed from the toluene fractions by oil pump vacuum to give a mixture of **12** and **13** (0.092 g) The solid was dissolved in CH_2Cl_2 and layered with methanol. A yellow powder precipitated overnight, which was collected by filtration and dried by oil pump vacuum to give **12** as a yellow solid (0.0390 g, 0.0208 mmol; 40%).

B. A round-bottom flask was charged with **4** (0.0697 g, 0.0752 mmol), KPF_6 (0.0152 g, 0.0825 mmol), *t*-BuOK (0.0092 g, 0.082 mmol), CuCl (0.0020 g, 0.0020 mmol), THF (10 mL), and methanol (10 mL). A Schlenk flask was charged with **13** (0.087 g, 0.0751 mmol) and CH_2Cl_2 (4 mL), and *n*-$Bu_4N^+F^-$ (0.023 mL, 1.0 M in THF, 5 wt % H_2O) was added with stirring. After 15 min, the solution derived from **4** was transferred via syringe to that derived from **13**. The mixture was stirred overnight. The precipitate was isolated by filtration, washed with ethanol, and dried by oil pump vacuum to give **12** as a yellow solid (0.0910 g, 0.0470 mmol; 63%), dec pt > 221° (gradual darkening, then melting). Anal. Calcd for $C_{103}H_{91}F_5P_4Pt_2$: C, 63.83; H, 4.73. Found: C, 63.03; H, 4.73. DSC:[38] endotherm with T_i, 91.6 °C; T_e, 110.8 °C; T_c, 132.3 °C; T_f, 138.1 °C; endotherm with T_i, 140.2 °C; T_e, 158.2 °C; T_c, 174.8 °C; T_f, 177.8 °C. TGA: weight loss 26%, 236−410 °C. NMR (δ, $CDCl_3$): ^{1}H 7.50−7.47 (m, 12H, *o* to P), 7.28−7.24 (m, 12H, *o* to P′), 7.06 (d, 12H, $^3J_{HH}$ = 7.2 Hz, *m* to P), 6.95 (d, 12H, $^3J_{HH}$ = 7.2 Hz, *m* to P′), 6.27 (d, $^3J_{HH}$ = 2H, 7.3 Hz, *o* to Pt), 6.02 (d, $^3J_{HH}$ = 7.1 Hz, 2H, *m* to Pt), 2.32 (s, 18H, CH_3 *p* to P), 2.22 (s, 18H, CH_3 *p* to P′), 1.93 (s, 3H, CH_3 *p* to Pt); ^{13}C{^{1}H}[40] 150.3 (t, $^2J_{CP}$ = 9.9 Hz, *i* to Pt), 145.7 (dm, $^1J_{CF}$ = 254.0 Hz, *o*-C_6F_5), 140.8 (s, *p* to P), 140.3 (s, *p* to P′), 139.1 (s, *o* to Pt), 134.6 (virtual t, $^2J_{CP}$ = 6.1 Hz,[41] *o* to P), 134.4 (virtual t, $^2J_{CP}$ = 6.3 Hz,[41] *o* to P′), 129.0 (s, *p* to Pt), 128.4 (virtual t, $^3J_{CP}$ = 5.3 Hz,[41] *m* to P), 128.2 (virtual t, $^3J_{CP}$ = 5.3 Hz,[41] *m* to P′), 127.7 (virtual t, $^1J_{CP}$ = 29.9 Hz,[41] *i* to P; *i* to P′ obscured), 127.5 (s, *m* to Pt), 109.9 (t, $^2J_{CP}$ = 15.2 Hz, *p*-tolPt*C*≡), 99.2 (s, PtC≡*C*), 98.4 (s, PtC≡*C*), 93.5 (br s, C_6F_5Pt*C*≡), 61.3 (s, PtC≡C*C*), 60.2 (s, PtC≡C*C*), 21.29 (s, CH_3 *p* to P), 21.27 (s, CH_3 *p* to P′), 20.5 (s, CH_3 *p* to Pt); ^{31}P{^{1}H} 18.7 (s, $^1J_{PPt}$ = 2955 Hz, $P_{p\text{-tol}}$),[39] 17.2 (s, $^1J_{PPt}$ = 2689 Hz, P_{C6F5}).[39] IR (cm^{-1}, powder film): $\nu_{C\equiv C}$ 2104 (m). UV−vis (CH_2Cl_2, 1.25 × 10^{-5} M):[42] 329 (32 100), 348 (14 800), 376 (8400). MS:[43] 1937 (M^+, 10%), 970 ([(C_6F_5)(tol$_3$P)$_2$Pt]$^+$, 20%), 894 ([(tol)(tol$_3$P)$_2$Pt]$^+$, 30%), 803 ([(tol$_3$P)$_2$Pt]$^+$, 100%).

***trans,trans*-(C_6F_5)(Et_3P)$_2$Pt(C≡C)$_3$Pt(PEt_3)$_2$(*p*-tol) (17).** A round-bottom flask was charged with **7** (0.113 g, 0.203 mmol), KPF_6 (0.041 g, 0.22 mmol), *t*-BuOK (0.0270 g, 0.243 mmol), CuCl (0.0040 g, 0.0040 mmol), THF (10 mL), and methanol (10 mL). A Schlenk flask was charged with *trans*-(C_6F_5)(Et_3P)$_2$Pt(C≡C)$_3$SiEt_3 (**15**;[7] 0.154 g, 0.203 mmol) and CH_2Cl_2 (4 mL), and *n*-$Bu_4N^+F^-$ (0.023 mL, 1.0 M in THF, 5 wt % H_2O) was added with stirring. After 15 min, the solution derived from **7** was transferred via syringe to that derived from **15**. The mixture was stirred overnight. The precipitate was isolated by filtration, washed with ethanol, and dried by oil pump vacuum to give **17** as a yellow solid (0.142 g, 0.120 mmol; 59%), dec pt > 211 °C (gradual darkening without melting). Anal. Calcd for $C_{43}H_{67}F_5P_4Pt_2$: C, 43.29; H, 5.66. Found: C, 42.26; H, 5.66. DSC: no features below 200 °C. TGA: weight loss 47%, 235−410 °C. NMR (δ, $CDCl_3$): ^{1}H 7.11 (d, 2H, $^3J_{HH}$ = 7.5 Hz, *o* to Pt), 6.78 (d, 2H, $^3J_{HH}$ = 7.5 Hz, *m* to Pt), 2.17 (s, 3H, CH_3 *p* to Pt), 1.78−1.67 (m, 24H, PCH_2CH_3 + P′CH_2CH_3), 1.10−1.02 (m, 36H, PCH_2CH_3 + P′CH_2CH_3); ^{13}C{^{1}H}[40] 150.3 (s, *i* to Pt), 138.9 (s, *o* to Pt), 130.6 (s, *p* to Pt), 128.6 (s, *m* to Pt), 109.2 (s, PtC≡), 93.3 (s, PtC≡*C*), 93.1 (s, PtC≡*C*), 60.8 (s, PtC≡C*C*), 60.7 (s, PtC≡C*C*), 20.9 (s, CH_3 *p* to Pt), 15.9 (virtual t, $^1J_{PC}$ = 17.5 Hz,[41] PCH_2), 15.3 (virtual t, $^2J_{PC}$ = 17.3 Hz,[41] P′CH_2), 8.1 (s, PCH_2CH_3), 8.0 (s, P′CH_2CH_3); ^{31}P{^{1}H} 13.1 (s, $^1J_{PPt}$ = 2406 Hz, P_{C6F5}),[39] 11.3 (s, $^1J_{PPt}$ = 2620 Hz, $P_{p\text{-tol}}$).[39] IR (cm^{-1}, powder film): $\nu_{C\equiv C}$ 2150 (ms), 2096 (vw), 2003 (w). UV−vis (CH_2Cl_2, 1.25 × 10^{-5} M):[42] 281 (53 600), 299 (34 900), 312 (39 600), 342 (9500), 367 (5400). MS:[43] 1192 (M^+, 100%), 597 ([(C_6F_5)(Et_3P)$_2$Pt]$^+$, 20%), 522 ([(tol)(Et_3P)$_2$Pt]$^+$, 60%).

***trans*-(C_6F_5)(Et_3P)$_2$Pt(C≡C)$_2$Au(PPh_3) (18).** A Schlenk flask was charged with **6** (0.100 g, 0.154 mmol), (Ph_3P)AuCl (0.076 g, 0.154 mmol),[21] and THF (5 mL) with stirring. Then KN($SiMe_3$)$_2$ (0.610 mL, 0.5 M in toluene, 0.305 mmol) was added. After 18 h, the volatiles were removed by oil pump vacuum. The residue was extracted with CH_2Cl_2 (2 × 2 mL). The extract was filtered through an alumina/Celite pad (2 × 1 cm). The solvent was removed by rotary evaporation and oil pump vacuum to give **18** as a yellow powder (0.166 g, 0.148 mol; 97%), dec pt > 190 °C (gradual darkening, then melting). Anal. Calcd for $C_{40}H_{45}AuF_5P_3Pt$: C, 43.45; H 4.10. Found: C, 43.76; H, 4.72. DSC:[38] endotherm with T_i, 104.0 °C; T_e, 107.6 °C; T_c, 120.6 °C; T_f, 123.3 °C; endotherm with T_i, 131.4 °C; T_e, 137.0 °C; T_c, 148.4 °C; T_f, 155.5 °C; endotherm with T_i, 185.2 °C; T_e, 191.1 °C; T_c, 202.9 °C; T_f, 205.6 °C. TGA: weight loss 38%, 206−404 °C. NMR (δ, $CDCl_3$): ^{1}H 7.48−7.37 (m, 15H, Ph), 1.73−1.71 (m, 12H, PCH_2), 1.04−0.96 (m, 18H, PCH_2CH_3); ^{13}C{^{1}H}[40] 146.8 (dm, $^1J_{CF}$ = 197 Hz, *o*-C_6F_5), 136.5 (dm, $^1J_{CF}$ = 197 Hz, *m*-C_6F_5), 134.2 (d, $^2J_{CP}$ = 13.8 Hz, *o* to P), 131.4 (br s, *p* to P), 129.8 (d, $^1J_{CP}$ = 55.6 Hz, *i* to P), 129.0 (d, $^3J_{CP}$ = 11.2 Hz,

(42) Absorptions are in nm (ε, M^{-1} cm^{-1}).

(43) FAB, 3-NBA: *m/z* for the most intense peak of the isotope envelope; relative intensities (%) are for the specified mass range.

m to P), 116.6 (d, $^2J_{CP}$ = 143.7 Hz, AuC≡), 93.7 (s, PtC≡), 91.9 (d, $^3J_{CP}$ = 30.2 Hz, AuC≡*C*), 90.6 (s, PtC≡*C*), 15.5 (virtual t, $^1J_{CP}$ = 17.5 Hz,[41] PCH_2), 7.8 (s, PCH_2CH_3); $^{31}P\{^1H\}$ 42.5 (s, PPh_3), 13.6 (s, $^1J_{PPt}$ = 2422 Hz, PEt_3).[39] IR (cm^{-1}, powder film): $\nu_{C\equiv C}$ 2146 (m), 2092 (w). UV−vis (CH_2Cl_2, 1.25 × 10^{-5} M; MTHF, see Table 5 and Figure 5):[42] 301 (56000), 358 (7200). MS:[43] 1565 ([M + $AuPPh_3$]$^+$, 100%), 1106 (M^+, 80%).

***trans*-$(C_6F_5)(Et_3P)_2Pt(C\equiv C)_2W(CO)_3(\eta^5\text{-}C_5H_5)$ (22).** A Schlenk flask was charged with *trans*-$(C_6F_5)(Et_3P)_2PtCl$ (**2**;[2] 0.234 g, 0.369 mmol), CuI (0.0070 g, 0.036 mmol), and $HNEt_2$ (20 mL) with stirring, and cooled to 0 °C. Then a solution of $(\eta^5\text{-}C_5H_5)(CO)_3W(C\equiv C)_2H$ (**23**;[25] 0.181 g, 0.472 mmol) in CH_2Cl_2 (5 mL) was added. The cold bath was allowed to warm to room temperature. After 20 h, the solvent was removed by oil pump vacuum. The tan residue was extracted with toluene (3 × 3 mL). The extracts were filtered through an alumina column (5 × 2 cm), which was rinsed with toluene. The solvent was removed by rotary evaporation. The residue was washed with ethanol (5 mL) and dried by oil pump vacuum to give **22** as a yellow solid (0.290 g, 0.295 mmol, 80%) of 80% purity by ^{31}P NMR. NMR (δ, $CDCl_3$): ^1H 5.59 (s, 5H, C_5H_5), 1.77−1.68 (m, 12H, PCH_2), 1.06−0.98 (m, 18H, PCH_2CH_3); $^{13}C\{^1H\}$[40] 211.0 (s, CO), 116.4 (s, W*C*≡), 93.9 (s, Pt*C*≡), 91.6 (s, C_5H_5), 68.1, 54.6 (2 s, WC≡*C*–*C*, tentative), 15.5 (virtual t, $^1J_{CP}$ = 17.5 Hz,[41] PCH_2), 7.8 (virtual t, $^2J_{CP}$ = 11.6 Hz,[41] PCH_2CH_3); $^{31}P\{^1H\}$ 12.8 (s, 80%, $^1J_{PPt}$ = 2431 Hz),[39] 9.8 (s, 16% (major byproduct), $^1J_{PPt}$ = 2427 Hz).[39] IR (cm^{-1}, powder film): $\nu_{C\equiv C}$ 2146 (w), 2084 (w), ν_{CO} 2034 (s), 1938 (s).

Crystallography. A CH_2Cl_2 solution of **8** was layered with methanol and refrigerated. After 1 week, white prisms of **8** were isolated. CH_2Cl_2 solutions of **9** and **17** were layered with hexanes. After 2 weeks, white prisms of **9**·CH_2Cl_2 and yellow prisms of **17** were isolated. A toluene solution of **18** was layered with ethanol. After 1 week, pale yellow plates of **18**·$(C_7H_8)_{0.5}$ were isolated. Data were collected using a Nonius KappaCCD detector as outlined in Table 3.

Cell parameters were obtained from 10 frames using a 10° scan and were refined with the following number of reflections: **8**, 4658; **9**·CH_2Cl_2, 30 543; **17**, 10 768; **18**·$(C_7H_8)_{0.5}$, 11 502. Lorentz, polarization, and absorption corrections were applied.[44] The space groups were determined from systematic absences and subsequent least-squares refinement. The structures were solved by direct methods. The parameters were refined with all data by full-matrix-least-squares on F^2 using SHELXL-97.[45] Non-hydrogen atoms were refined with anisotropic thermal parameters. The hydrogen atoms were fixed in idealized positions using a riding model. Scattering factors were taken from the literature.[46]

The structure of **8** was disordered over two positions with a nearly perfect overlay of the C_6F_5 and the *p*-tolyl ligands. The occupancy refined to 73:27. However, the *p*-methyl and *p*-fluorine substituents could not be refined separately (F14/C14a; F84/C84a). Some of the PCH_2 carbon atoms of **9**·CH_2Cl_2 were also disordered and refined to occupancy ratios of 61:39 (C101/C111, C105/C115) and 44:56 (C104/C114). The toluene molecule in **18**·$(C_7H_8)_{0.5}$ was disordered and refined to 50% occupancy.

Acknowledgment. We thank the U.S. National Science Foundation (J.A.G., CHE-0719267; K.S.S., CHE-0515066), the Deutsche Forschungsgemeinschaft (SFB 583), and Johnson Matthey (platinum loans) for support.

Supporting Information Available: CIF files with crystallographic data for **8**, **9**, **17**, and **18**. This material is available free of charge via the Internet at htpp://pubs.acs.org.

OM800493X

(44) (a) *Collect* data collection software; Nonius B.V., 1998. (b) *Scalepack* data processing software: Otwinowski, Z.; Minor, W. in *Methods Enzymol.* **1997**, *276*, 307.

(45) Sheldrick, G. M. *SHELX-97*, Program for refinement of crystal structures; University of Göttingen, 1997.

(46) Cromer, D. T.; Waber, J. T. In *International Tables for X-ray Crystallography*; Ibers, J. A., Hamilton, W. C., Eds.; Kynoch: Birmingham, England, 1974.